

Electroweak transverse response functions in the GFMC framework

Alessandro Lovato

In collaboration with:

Omar Benhar, Stefano Gandolfi, Joe Carlson, Steve Pieper, Noemi Rocco, and Rocco Schiavilla

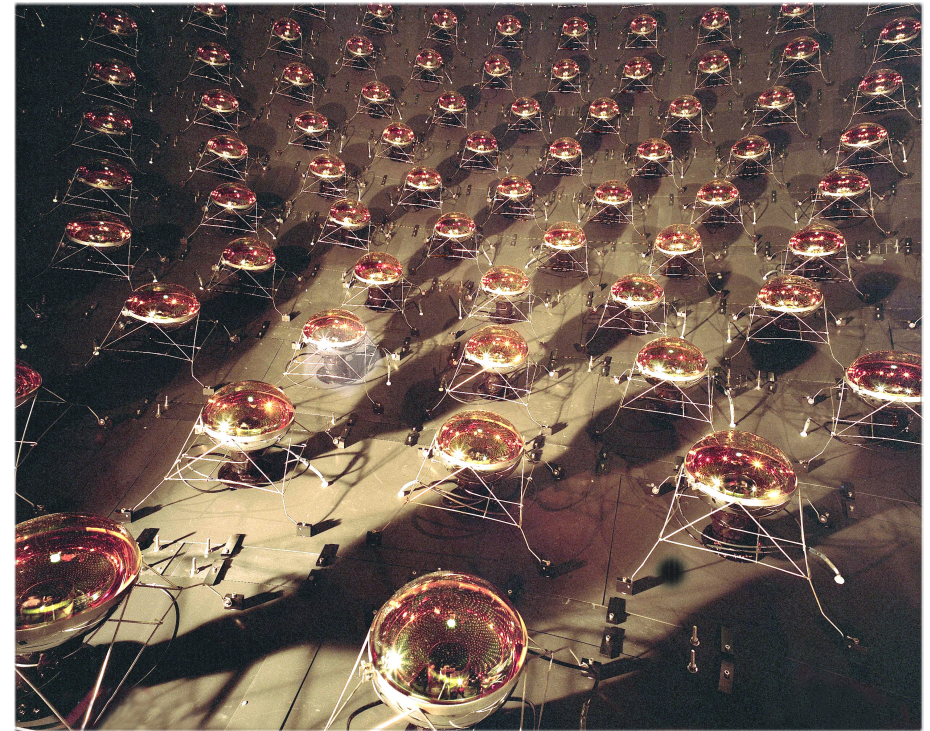


Introduction

- The electroweak response is a fundamental ingredient to describe neutrino-nucleus scattering.
- Neutrino experimental communities need accurate theoretical calculations

AND

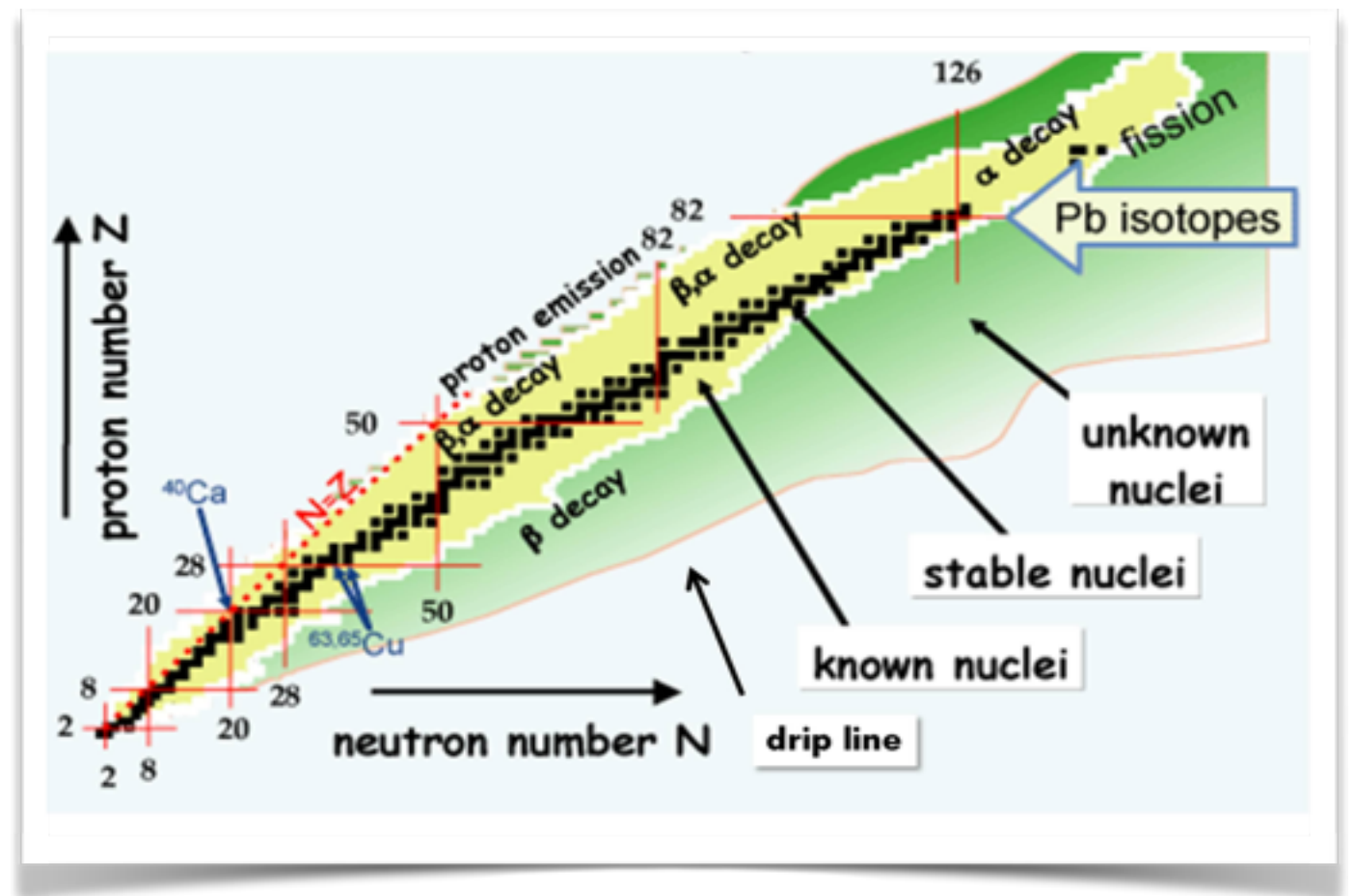
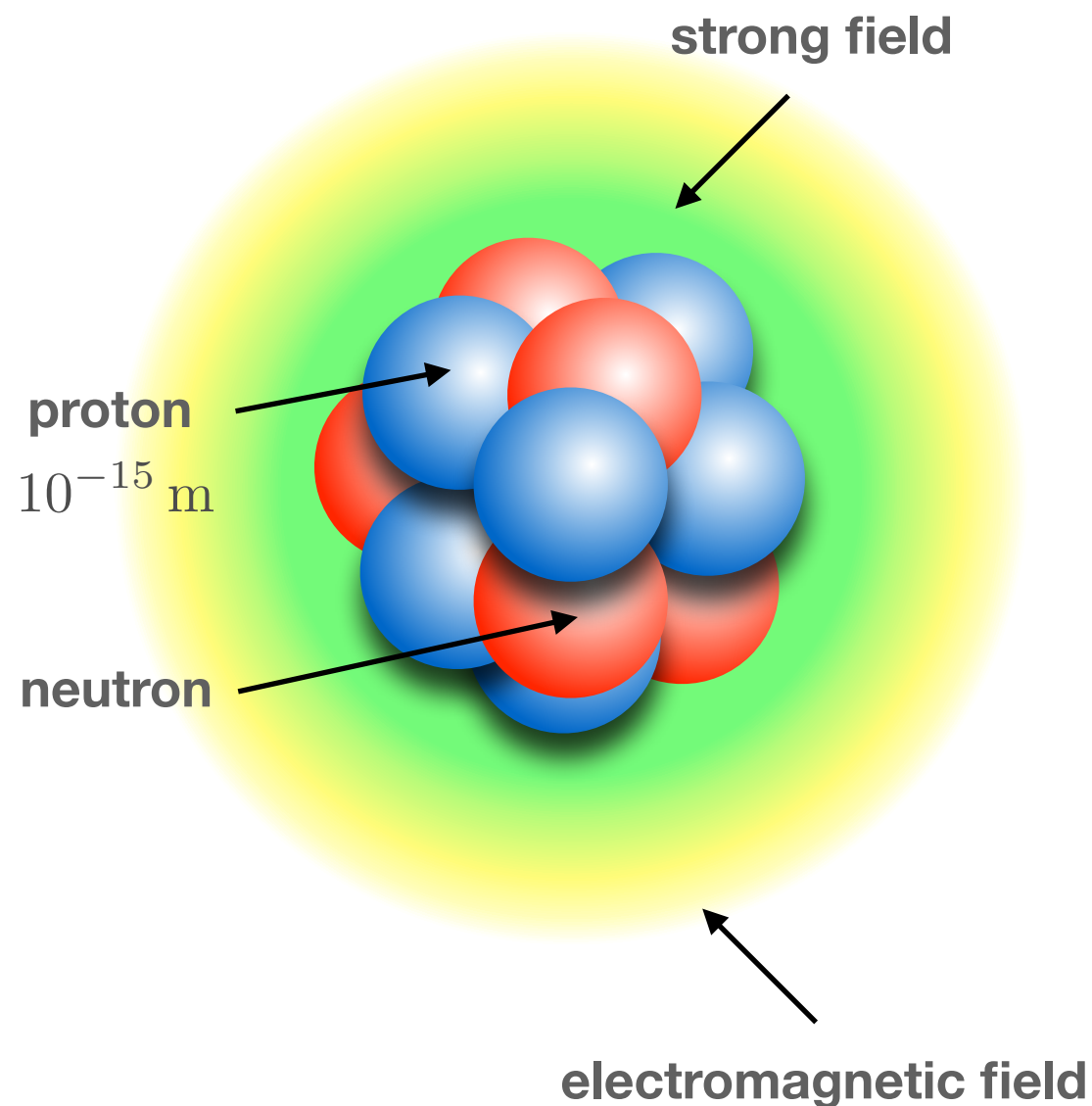
Reliable theoretical uncertainty estimates



- A large body of experimental data for the electromagnetic response of ^4He and ^{12}C (and larger nuclei) is available.
- A model unable to describe electron-nucleus scattering is (very) unlikely to describe neutrino-nucleus scattering.

Nuclear Physics in a Nutshell

- The goal of nuclear theory is understanding the structure, reactions and electroweak properties of atomic nuclei in terms of the interactions among their constituents.

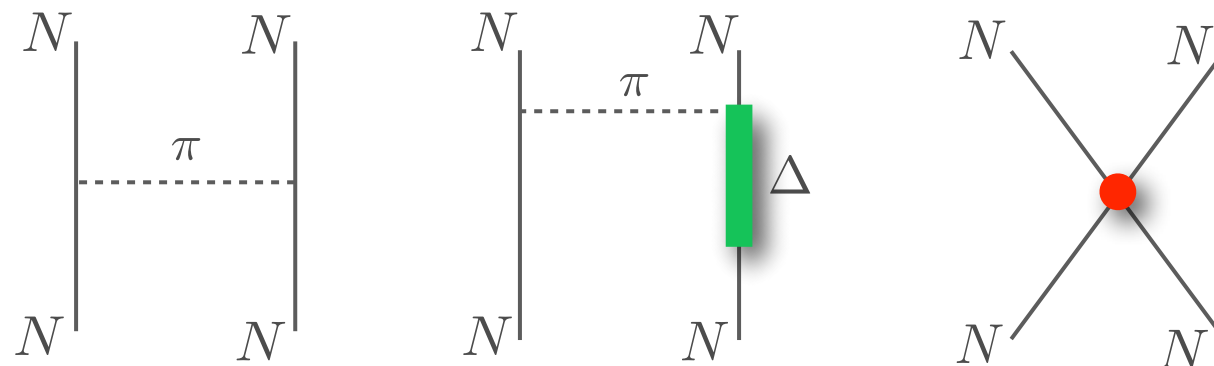


The nuclear Hamiltonian

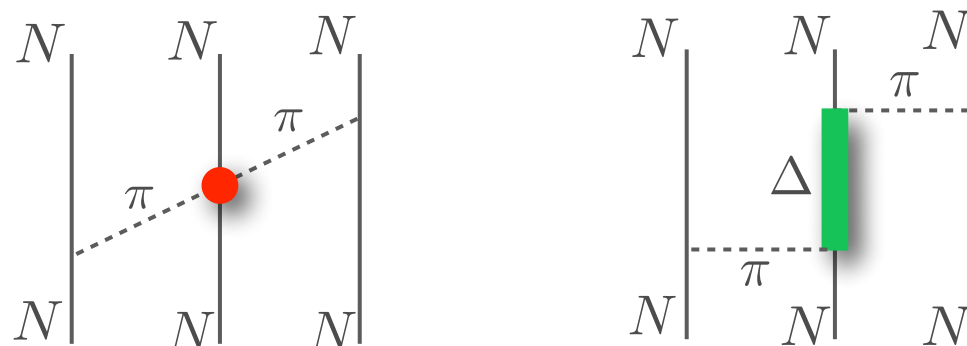
- Ab initio approaches are based on the non relativistic hamiltonian

$$H = \sum_i \frac{\mathbf{p}_i^2}{2m} + \sum_{i<j} v_{ij} + \sum_{i<j<k} V_{ijk} + \dots$$

The Argonne v₁₈ is a finite, local, configuration-space potential controlled by ~4300 np and pp scattering data below 350 MeV of the Nijmegen database



Three-nucleon interactions effectively include the lowest nucleon excitation, the $\Delta(1232)$ resonance, and other nuclear effects



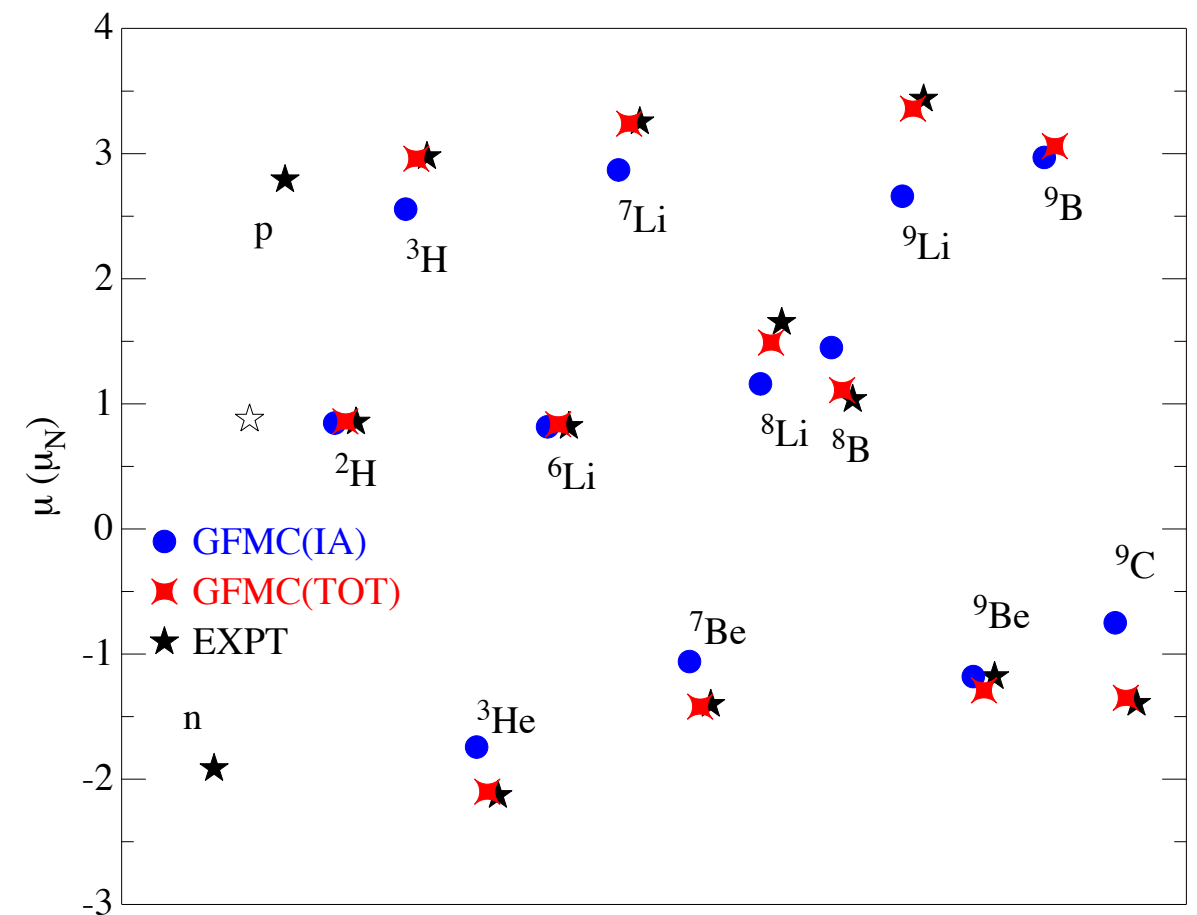
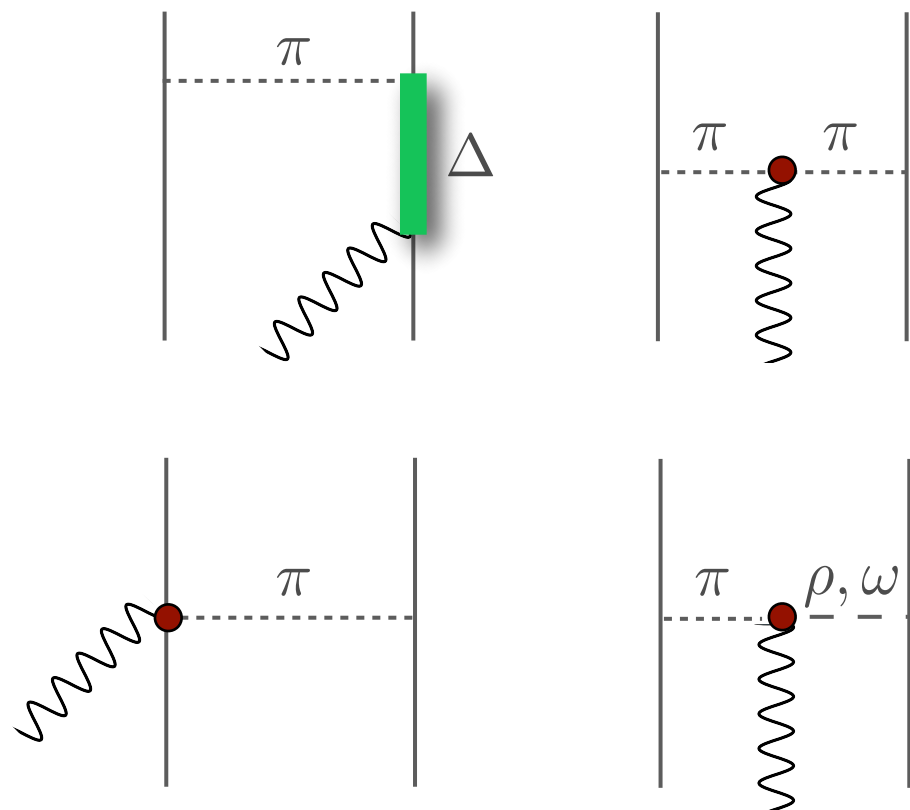
Nuclear currents

The nuclear electromagnetic current is constrained by the Hamiltonian through the continuity equation

$$\nabla \cdot \mathbf{J}_{\text{EM}} + i[H, J_{\text{EM}}^0] = 0$$

- The above equation implies that \mathbf{J}_{EM} involves two-nucleon contributions.

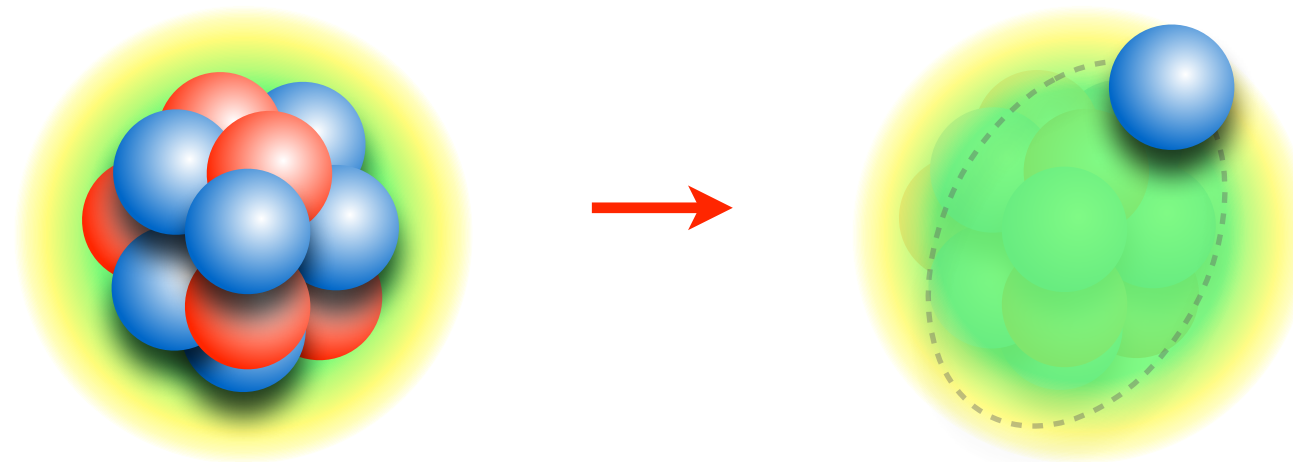
- They are essential for low-momentum and low-energy transfer transitions.



S. Pastore et al., PRC 87, 035503 (2013)

Mean field models

- Within mean field theories, nucleons are independent particles subject to an average potential generated by the other nucleons



$$\left[\sum_{i < j} v_{ij} + \sum_{i < j < k} V_{ijk} \right] \rightarrow \sum_i U_i$$

- * The average procedure depends upon the (large) system of interest
- * The interaction is usually fitted on nuclear binding energies and on low momentum observables
- * Nucleon-nucleon scattering data and deuteron properties are ignored
- * Not clear way to derive effective currents

Many-body wave function

Non relativistic many body theory is aimed at solving the Schrödinger equation

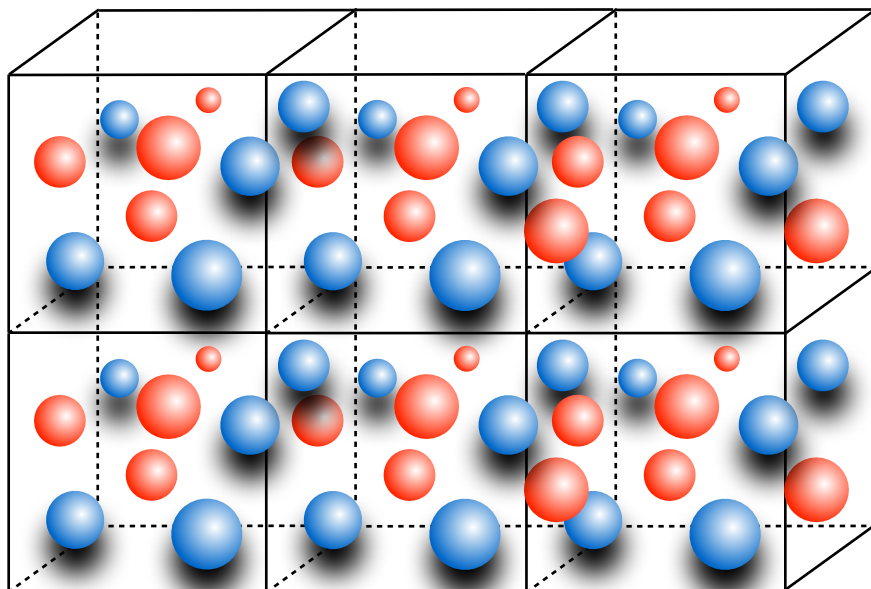
$$H\Psi_n(x_1, \dots, x_A) = E_n\Psi_n(x_1, \dots, x_A)$$

Within mean field approaches, the ground-state wave function is a Slater determinant of single particle waves functions

$$\Phi_0(x_1, \dots, x_A) = \mathcal{A}[\phi_{n_1}(x_1) \dots \phi_{n_A}(x_A)]$$

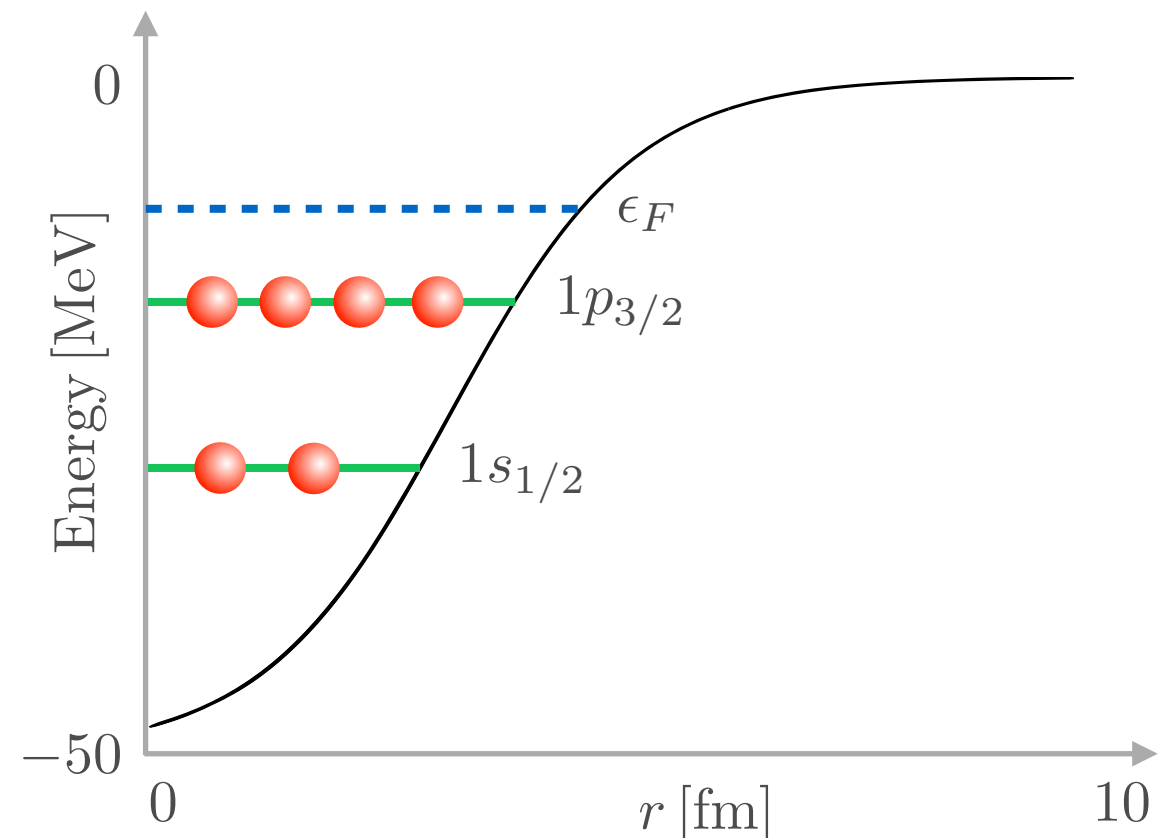
Infinite nuclear matter

- Single-particle wave functions are plane waves
- Box with periodic boundary conditions



Finite nuclei

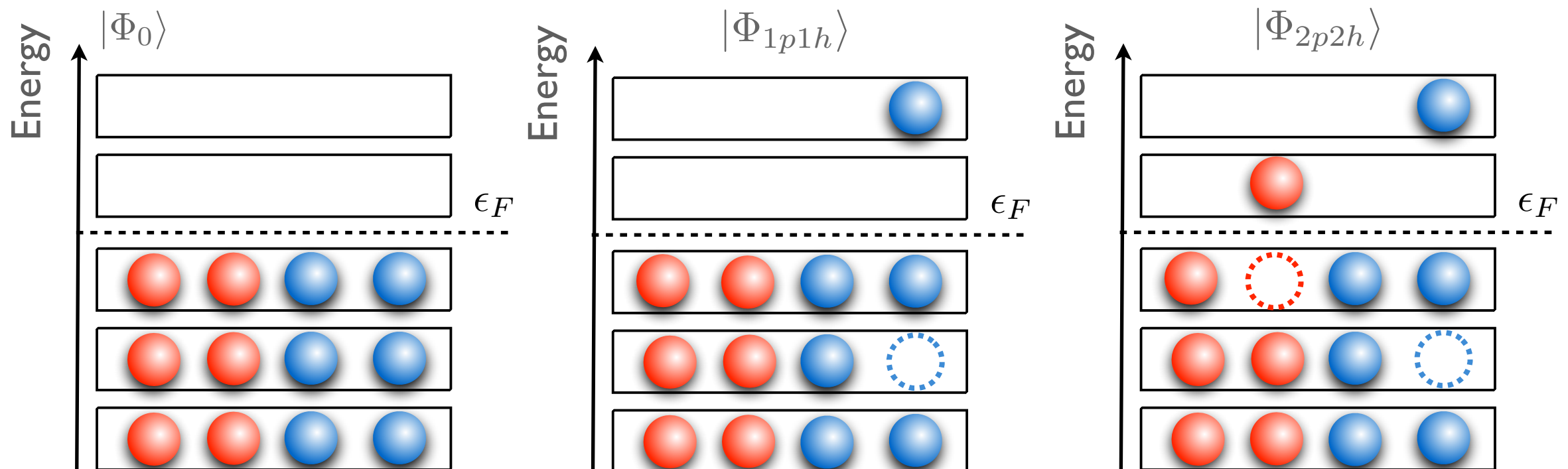
- Hartree-Fock solution



Many-body wave function

Excited states are constructed removing n occupied states from the Slater determinant and replacing them with n virtual (unoccupied) states

$$\Phi_{p_i, h_i}(x_1 \dots x_A) = \mathcal{A}[\phi_{n_1}(x_1) \dots \phi_{p_i}(x_i) \dots \phi_{n_A}(x_A)]$$



The eigenstate of the Hamiltonian is a linear combination of n -particles n -holes states

$$|\Psi_n\rangle = \sum c_{p_i, h_i}^n |\Phi_{p_i, h_i}\rangle \quad H|\Psi_n\rangle = E_n |\Psi_n\rangle$$

Many-body wave function

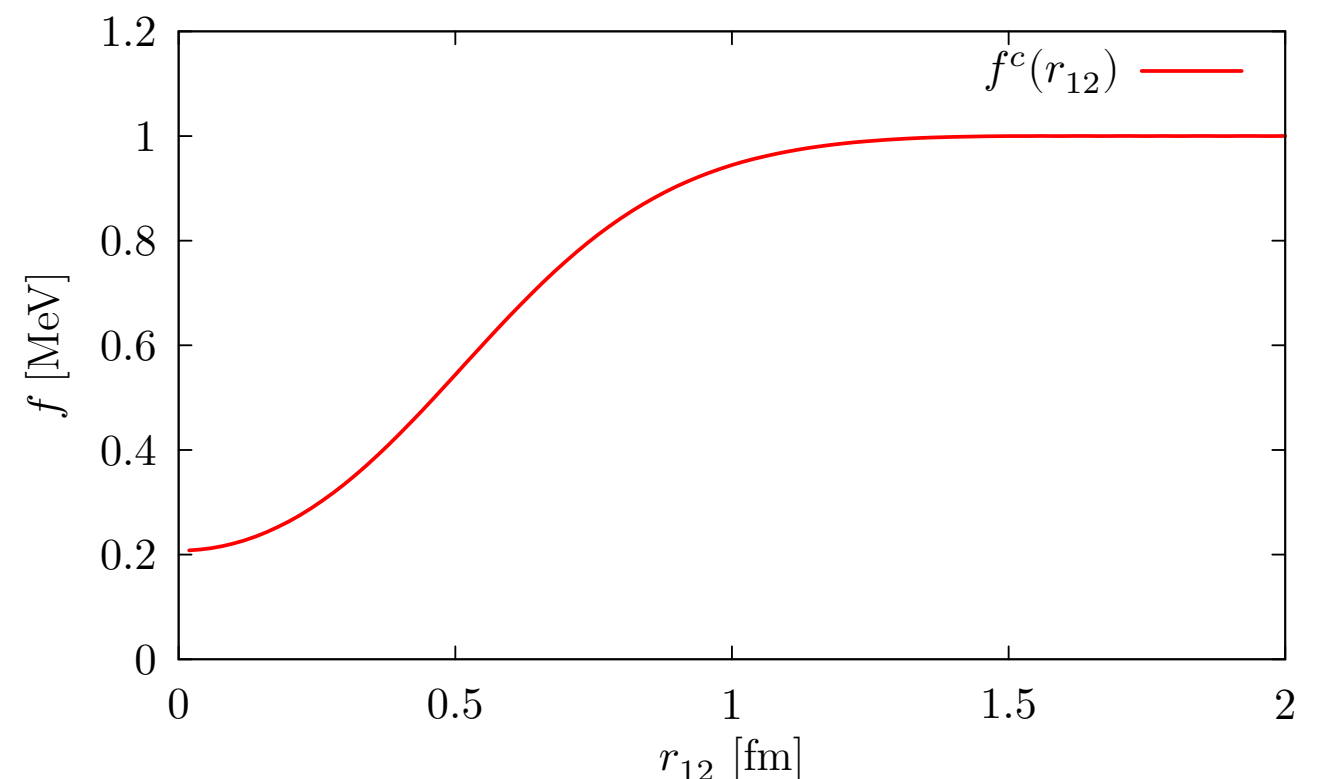
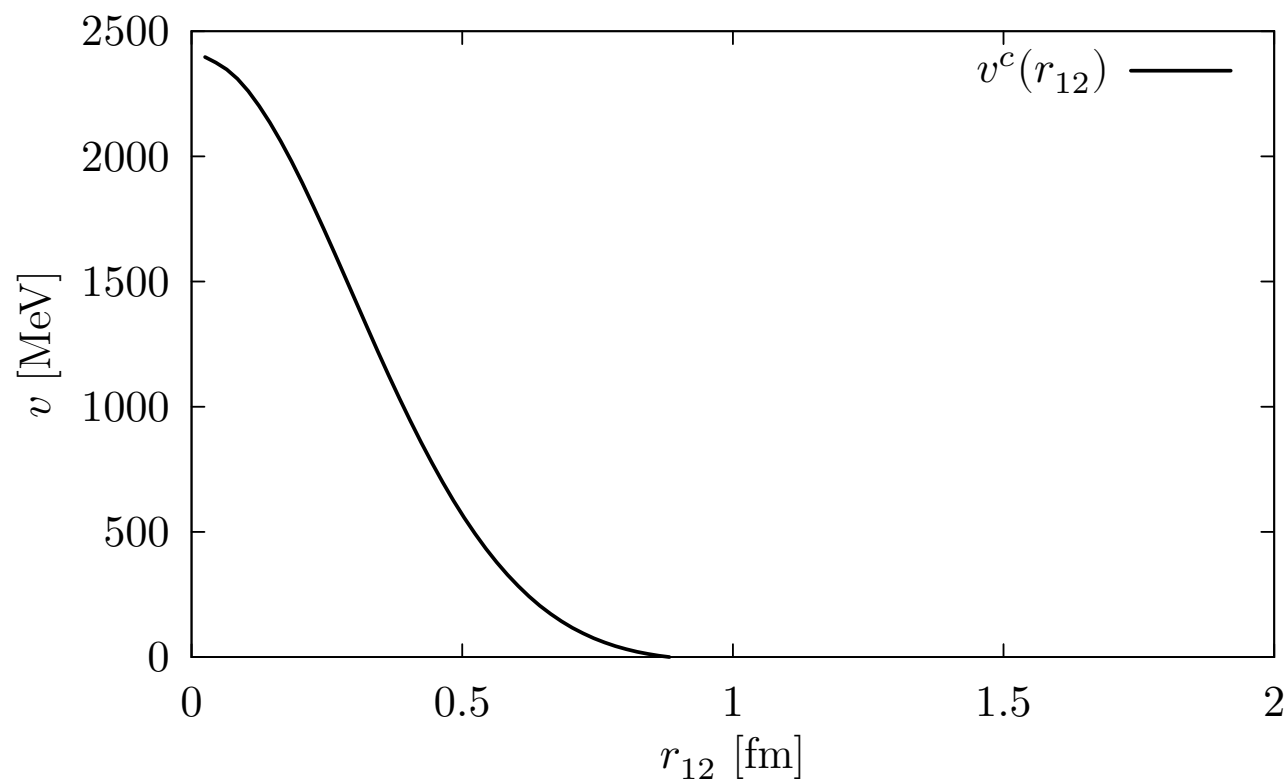
We explicitly account for the correlations induced by the nuclear interactions

$$\Phi_n(x_1 \dots x_A) \longrightarrow \mathcal{F} \Phi_n(x_1 \dots x_A)$$

The correlation operator reflects the spin-isospin dependence of the nuclear interaction

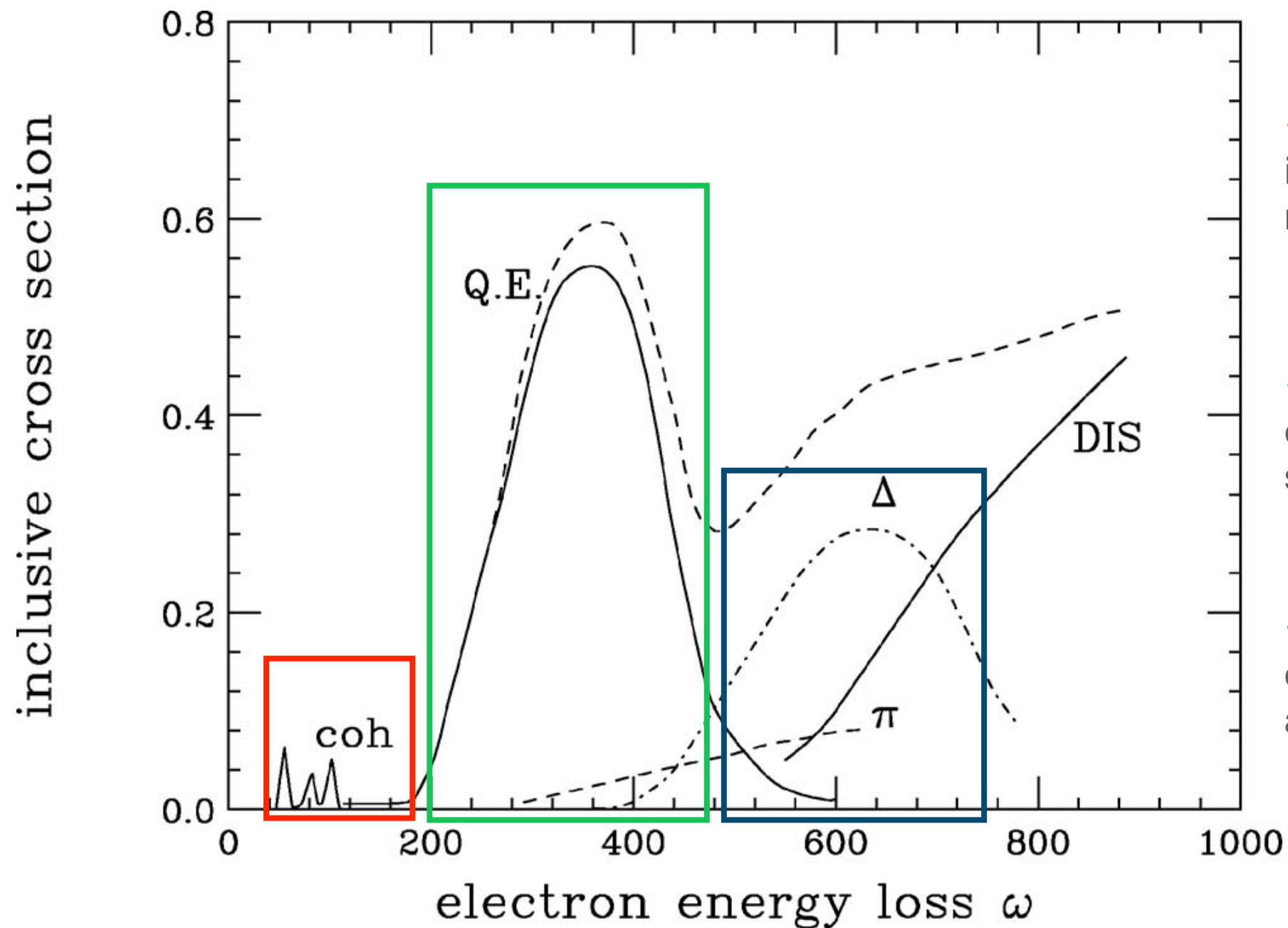
$$\mathcal{F} \equiv \left(\mathcal{S} \prod_{i < j} F_{ij} \right) \quad F_{ij} \equiv \sum_p f_{ij}^p O_{ij}^p$$

The shape of f_{ij}^p is determined by minimizing the variational energy $E_V \simeq \langle \Phi_0 | \mathcal{F}^\dagger H \mathcal{F} | \Phi_0 \rangle$



Electron-nucleus scattering

Schematic representation of the inclusive cross section as a function of the energy loss.



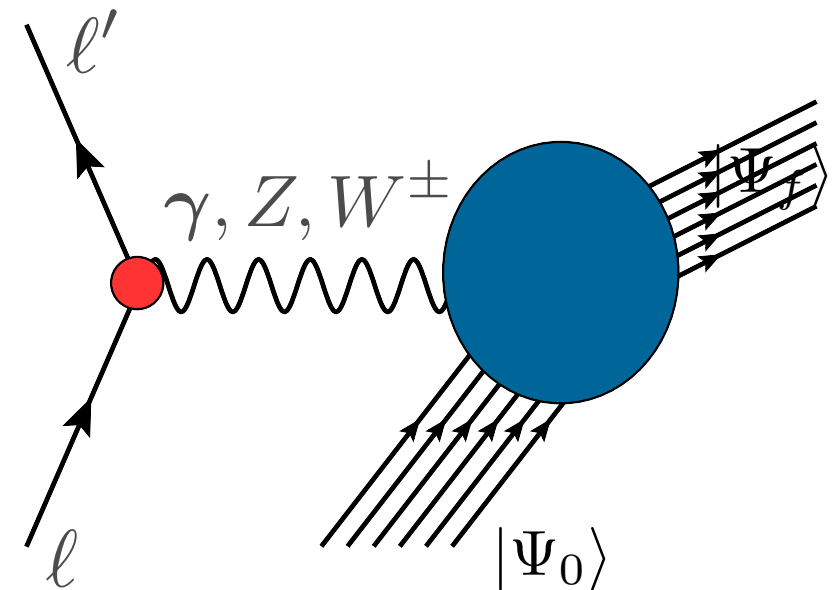
- Elastic scattering and inelastic excitation of discrete nuclear states.
- Broad peak due to quasi-elastic electron-nucleon scattering.
- Excitation of the nucleon to distinct resonances (like the Δ) and pion production.

Lepton-nucleus scattering

The inclusive cross section of the process in which a lepton scatters off a nucleus can be written in terms of five response functions

$$\frac{d\sigma}{dE_{\ell'} d\Omega_{\ell'}} \propto [v_{00}R_{00} + v_{zz}R_{zz} - v_{0z}R_{0z} + v_{xx}R_{xx} \mp v_{xy}R_{xy}]$$

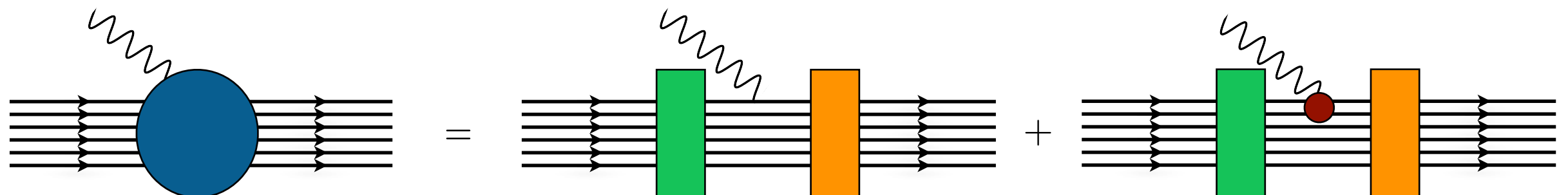
- In the electromagnetic case only the longitudinal and the transverse response functions contribute



- The response functions contain all the information on target structure and dynamics

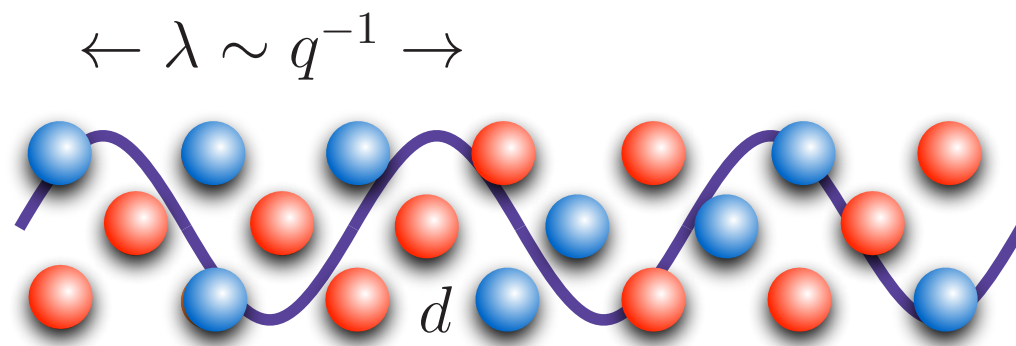
$$R_{\alpha\beta}(\omega, \mathbf{q}) = \sum_f \langle \Psi_0 | J_{\alpha}^{\dagger}(\mathbf{q}) | \Psi_f \rangle \langle \Psi_f | J_{\beta}(\mathbf{q}) | \Psi_0 \rangle \delta(\omega - E_f + E_0)$$

- They account for initial state correlations, final state correlations and two-body currents



Lepton-nucleus scattering

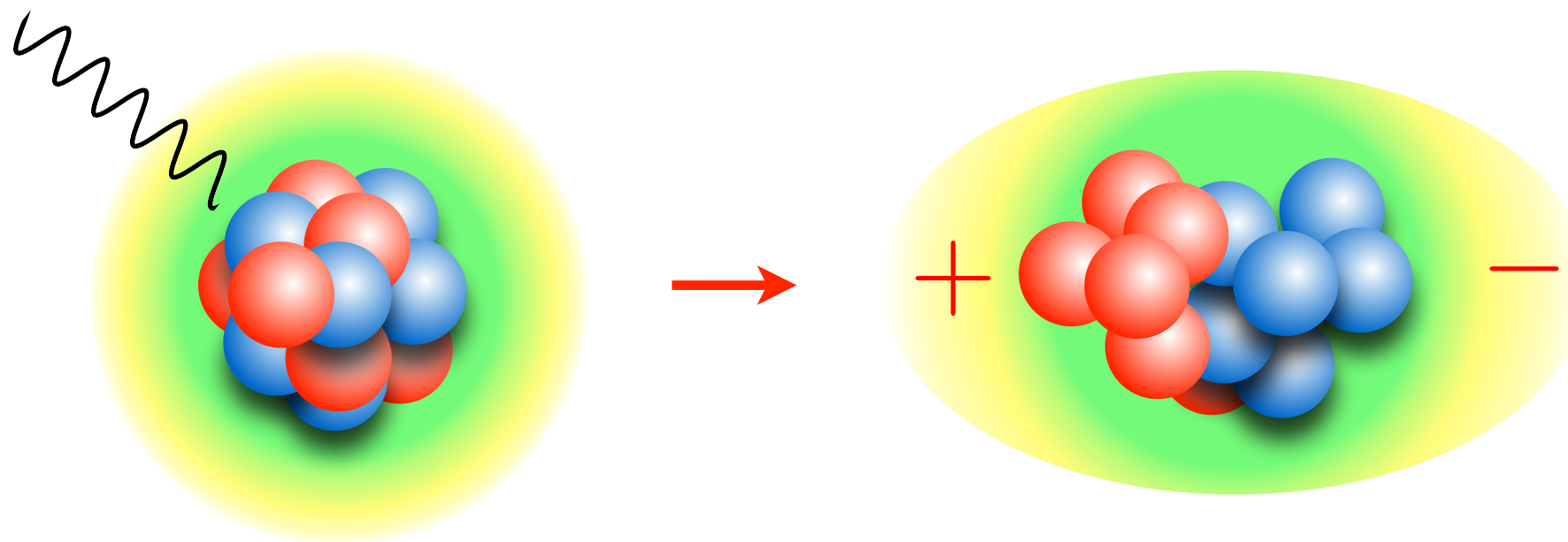
- At low momentum transfer the space resolution of the lepton becomes much larger than the average NN separation distance (~ 1.5 fm).
- In this regime the interaction involves many nucleons \longrightarrow long-range correlations, RPA



$$|\Psi_f\rangle = \sum c_{1p,1h}^f |\Psi_{1p1h}\rangle$$

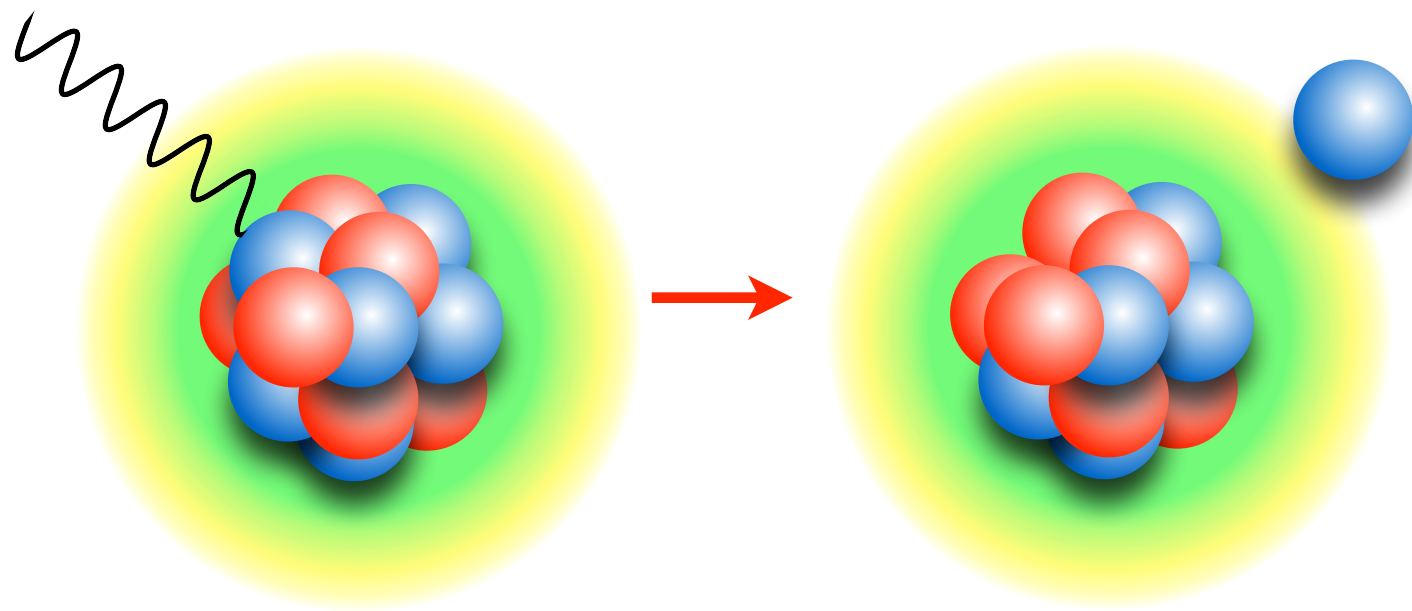
$$H^{\text{eff}} |\Psi_f\rangle = E_f |\Psi_f\rangle$$

- The giant dipole resonance is a manifestation of long-range correlations



Lepton-nucleus scattering

- At (very) large momentum transfer, scattering off a nuclear target reduces to the incoherent sum of scattering processes involving individual bound nucleons \longrightarrow short-range correlations.



$$|\Psi_f\rangle = |p\rangle \otimes |\Psi_f\rangle_{A-1}$$

$$|\Psi_f\rangle_{A-1} \approx \mathcal{F}|\Phi\rangle_{A-1}$$

- Relativistic effects play a major role and need to be accounted for along with nuclear correlations
- Resonance production and deep inelastic scattering also need to be accounted for

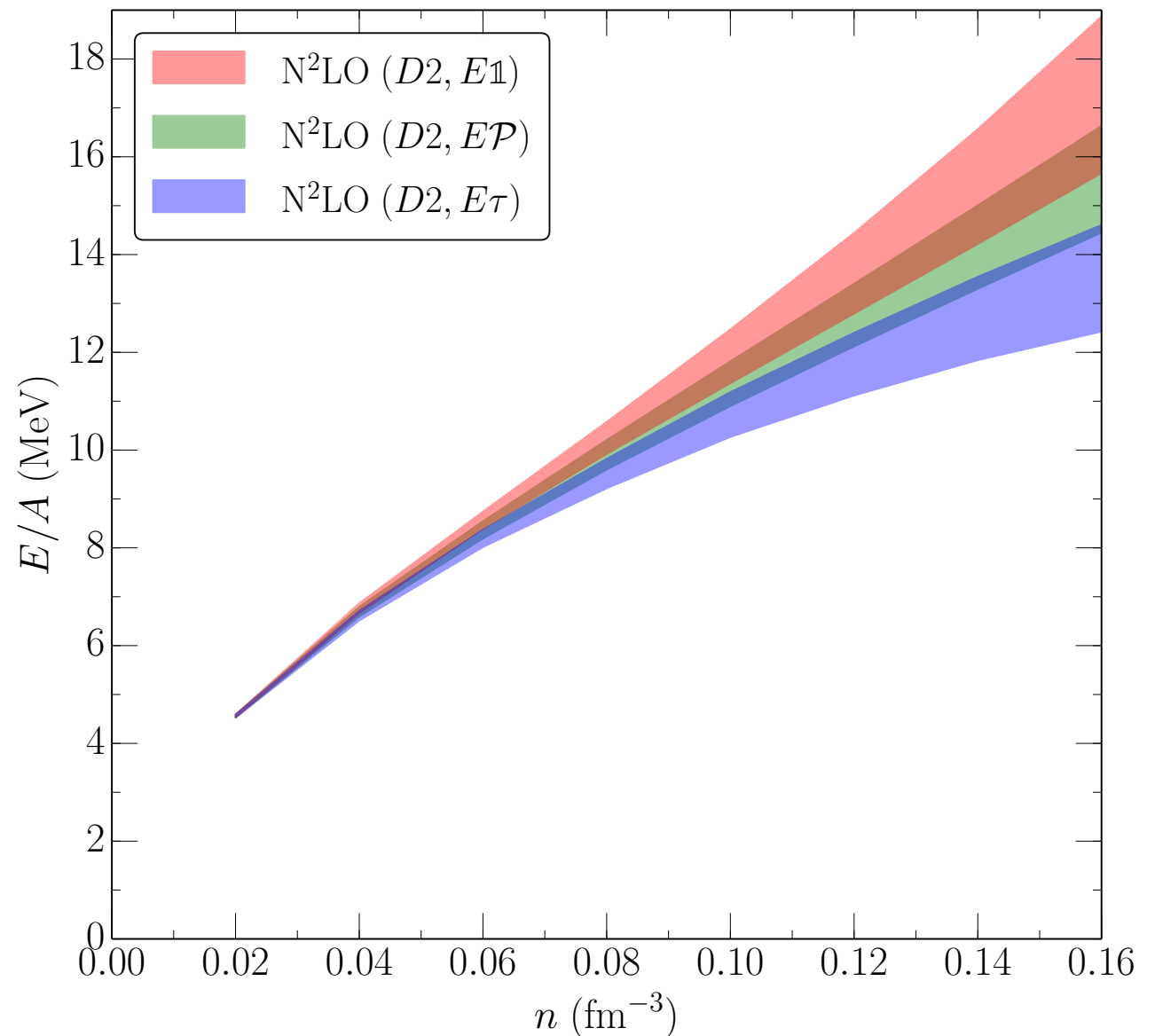
The goal (the dream)

We are aimed at computing the response functions of ^{12}C in the broad kinematical region covered by neutrino experiments along with a realistic estimate of the theoretical uncertainty of the calculation.

Sources of theoretical uncertainty

- Modeling nuclear dynamics: nuclear potential, currents, form factors...
- Many-body technique: quantum Monte Carlo spectral function

In ab initio approaches these two sources of theoretical uncertainty are disentangled and can be properly estimated



J. Lynn et al. PRL 116, 062501 (2016)

Our strategy: ab initio methods

Green's function Monte Carlo (GFMC)

- Virtually exact up to the quasielastic region for $q \lesssim 500\text{MeV}$
- Limited to nuclei large as ^{12}C
- Relativistic kinematic can be implemented but **A LOT OF WORK**

Auxiliary field diffusion Monte Carlo (AFDMC)

- Can be used to treat nuclei like ^{40}Ar (and bigger!) as well as nuclear matter
- Difficulties in extracting the response functions due to the large sign problem
- Relativistic kinematic can be implemented but again **A LOT OF WORK**

Spectral function

- Fully relativistic kinematics and matrix elements for the current operators
- Reliable only for relatively large momentum transfer: $q \gtrsim 300 \text{ MeV}$

Moderate momentum transfer

Quantum Monte Carlo

- The **diffusion Monte Carlo** methods use a projection technique to enhance the true ground-state component of a starting trial wave function.
- The trial wave function can be expanded in the complete set of eigenstates of the hamiltonian

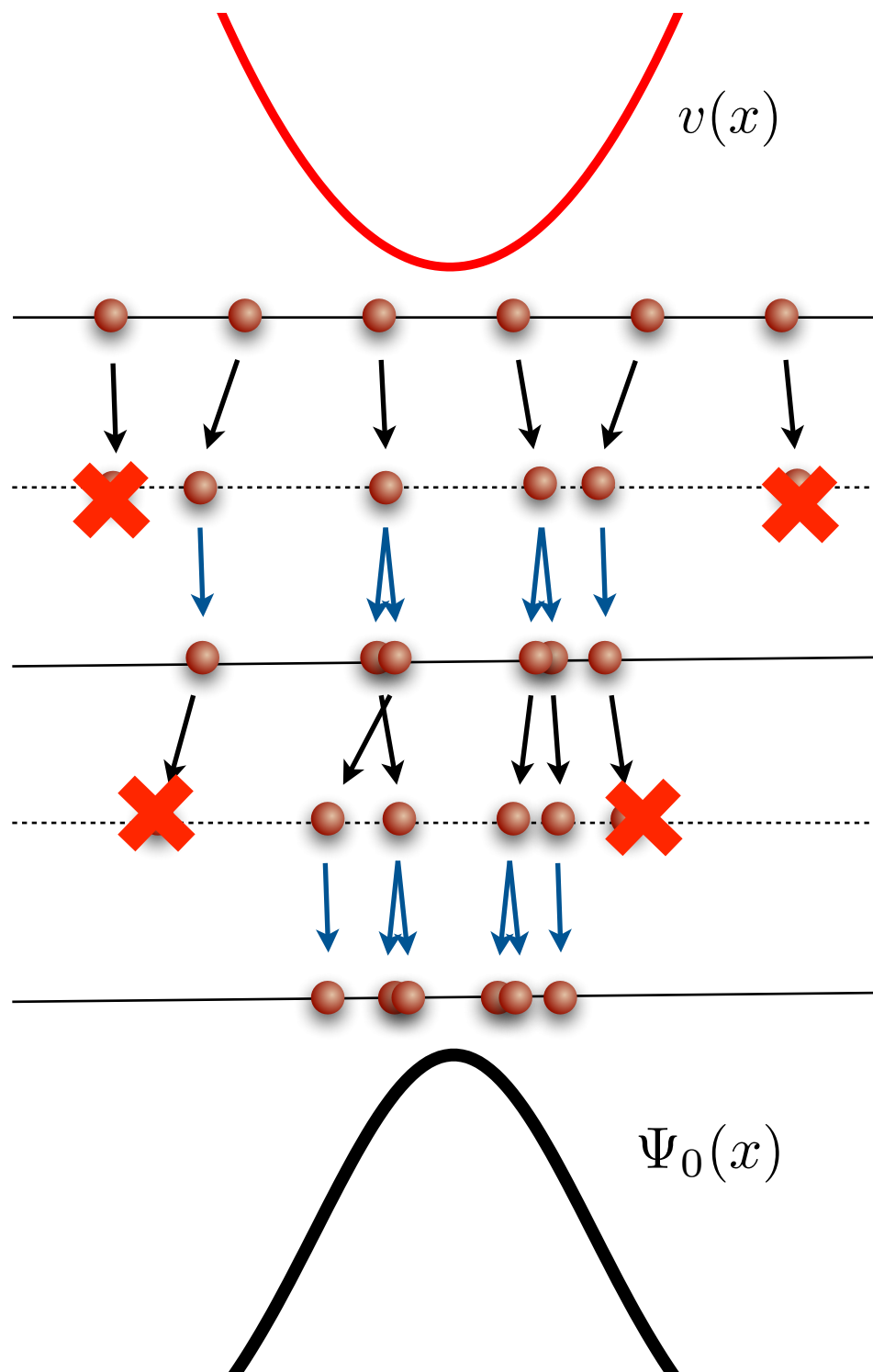
$$|\Psi_T\rangle = \mathcal{F}|\Phi_0\rangle \quad |\Psi_T\rangle = \sum_n c_n |\Psi_n\rangle \quad H|\Psi_n\rangle = E_n |\Psi_n\rangle$$

which implies the following imaginary time evolution

$$\lim_{\tau \rightarrow \infty} e^{-(H-E_0)\tau} |\Psi_T\rangle = \lim_{\tau \rightarrow \infty} \sum_n c_n e^{-(E_n-E_0)\tau} |\Psi_n\rangle = c_0 |\Psi_0\rangle$$

- Diffusion Monte Carlo can be applied to extract excited-states properties, but it is more difficult

Quantum Monte Carlo



- A set of walkers is sampled from the trial wave function

- Gaussian drift for the kinetic energy

$$\left(\frac{m}{2\pi\hbar^2\Delta\tau}\right)^{\frac{1}{2}} e^{-\frac{m}{2\hbar^2\Delta\tau}(x_i-x_{i+1})^2}$$

- Branching and killing of the walkers induced by the potential weight

$$w(x_{i+1}) = e^{-[V(x_{i+1})-E_0]\Delta\tau}$$

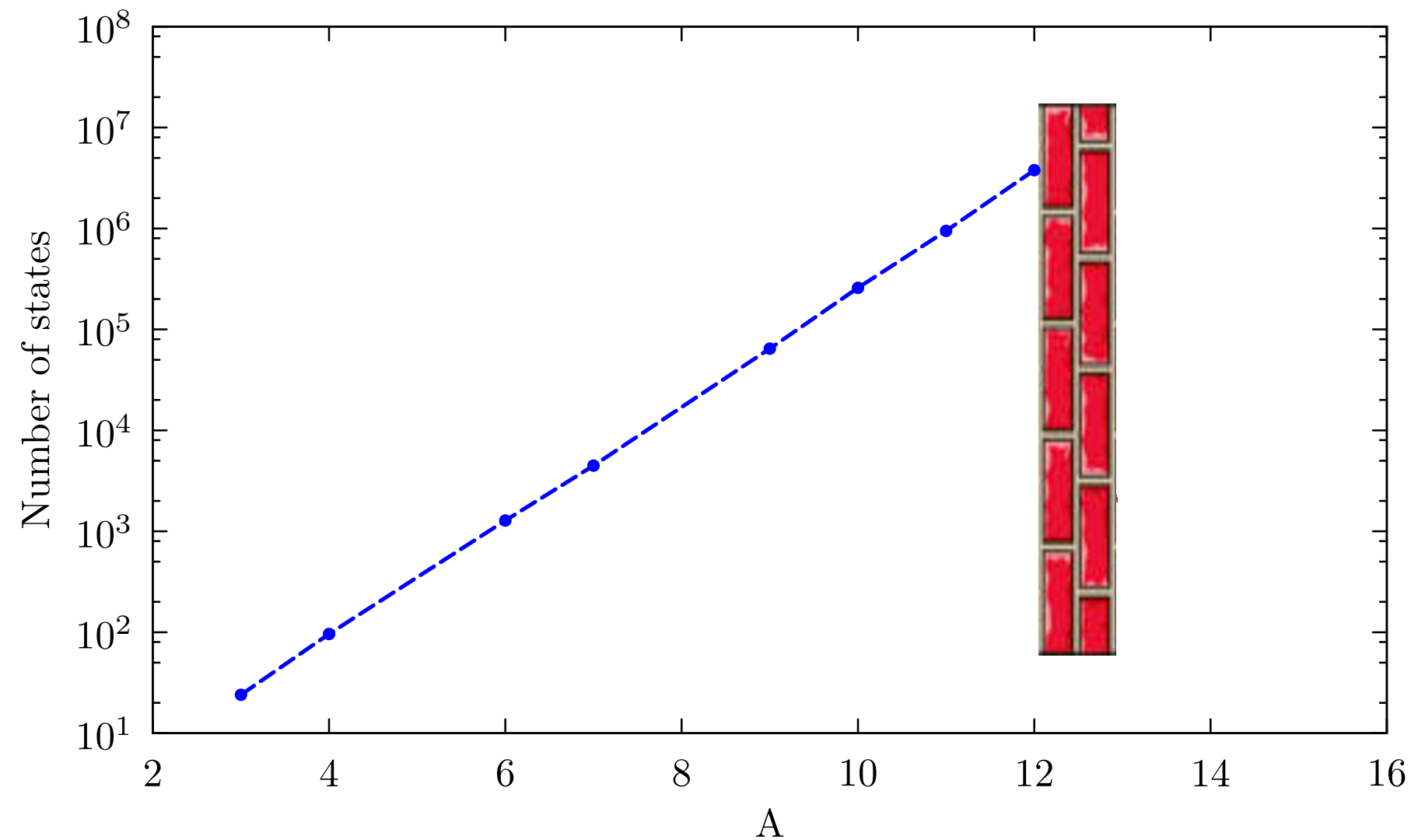
- Ground-state expectation values are estimated during the diffusion

$$\langle H \rangle = \frac{\sum_{x_i} \langle x_i | H | \Psi_T \rangle w(x_i)}{\sum_{x_i} \langle x_i | \Psi_T \rangle w(x_i)}$$

Quantum Monte Carlo

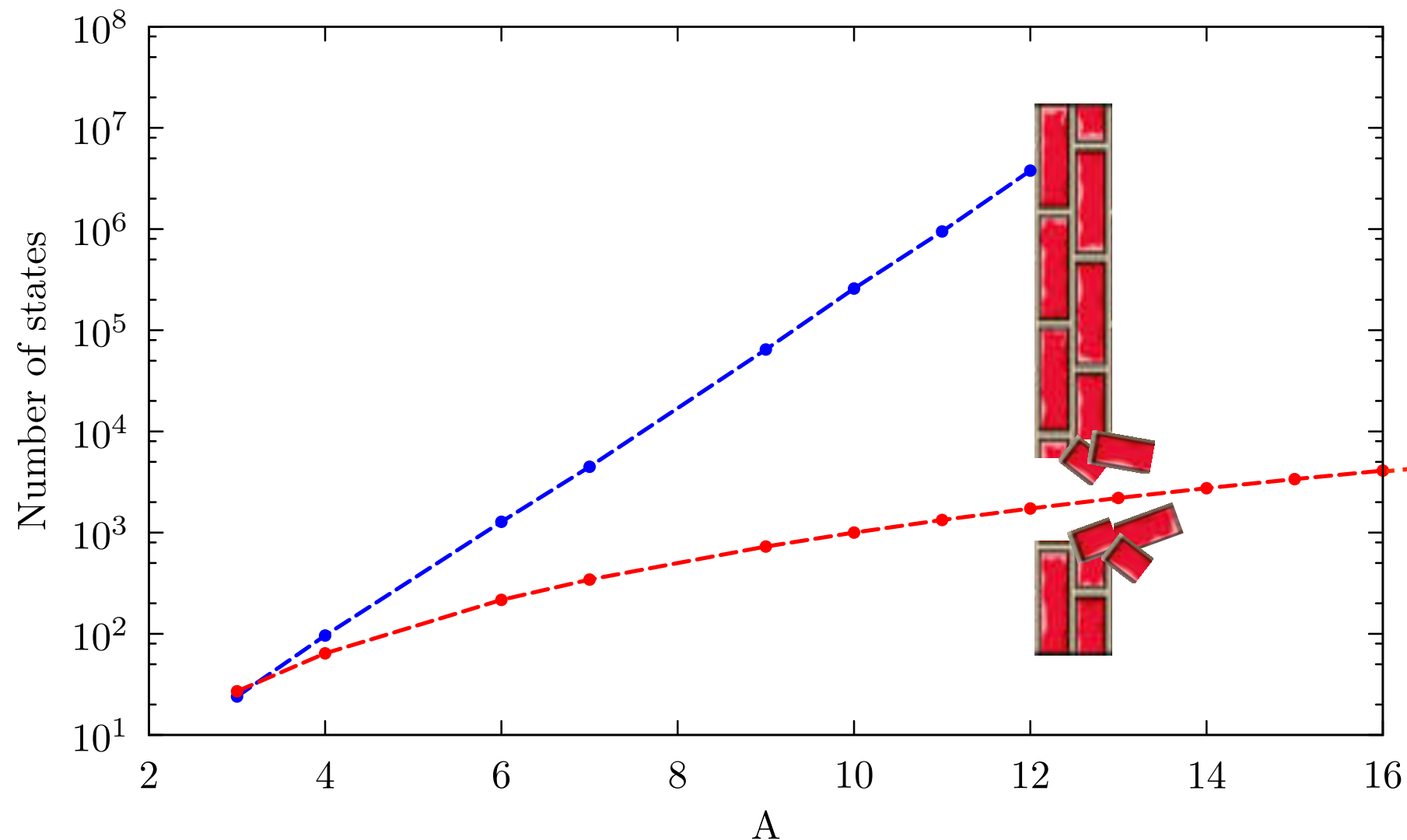
- **Green's function Monte Carlo (GFMC)** explicitly sums over the spin-isospin degrees of freedom

* Very accurate but limited to ^{12}C



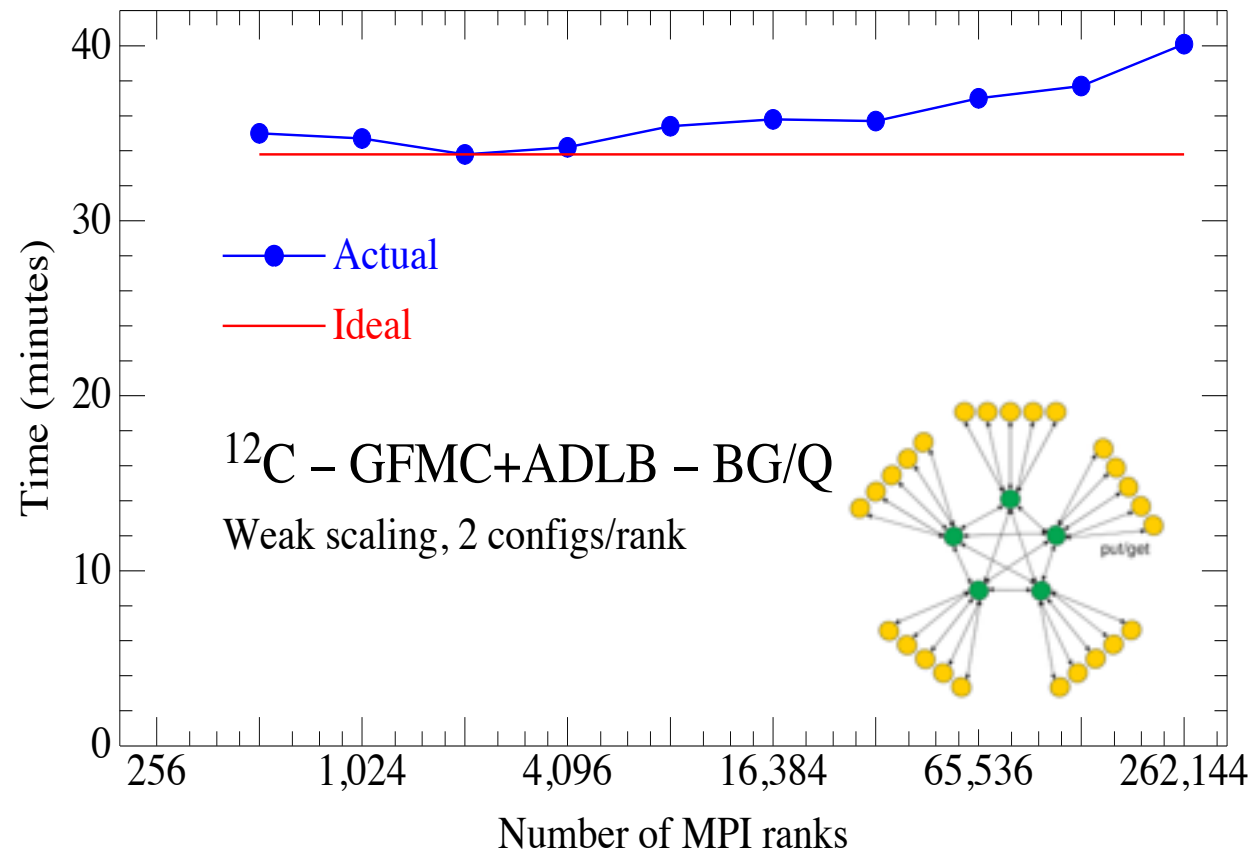
Quantum Monte Carlo

- **Green's function Monte Carlo (GFMC)** explicitly sums over the spin-isospin degrees of freedom
 - * Very accurate but limited to ^{12}C
- **Auxiliary field diffusion Monte Carlo (AFDMC)** samples the spin-isospin degrees of freedom
 - * Medium-mass nuclei, infinite (isospin-symmetric and asymmetric) nuclear matter



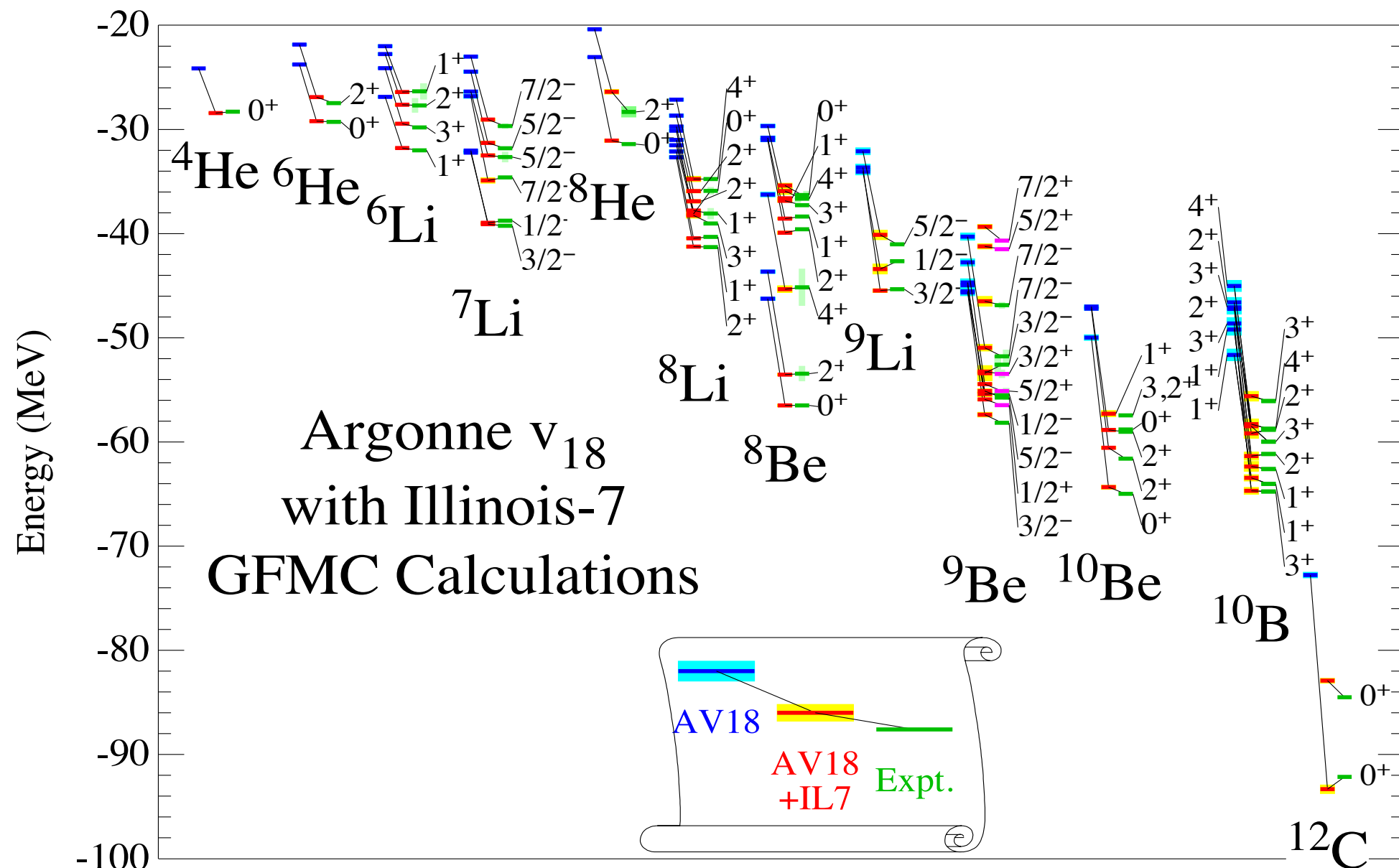
Quantum Monte Carlo

- Joint efforts between physicists and computing scientists have proven to be essential for most of the recent advances nuclear theory and extremely useful to attract the best students to the field
- GFMC has steadily undergone development to take advantage of each new generation of parallel machine and was one of the first to deliver new scientific results each time.



Quantum Monte Carlo

- Green's function Monte Carlo combined with a realistic nuclear hamiltonian reproduces the spectrum of ground- and excited states of light nuclei



Euclidean response function

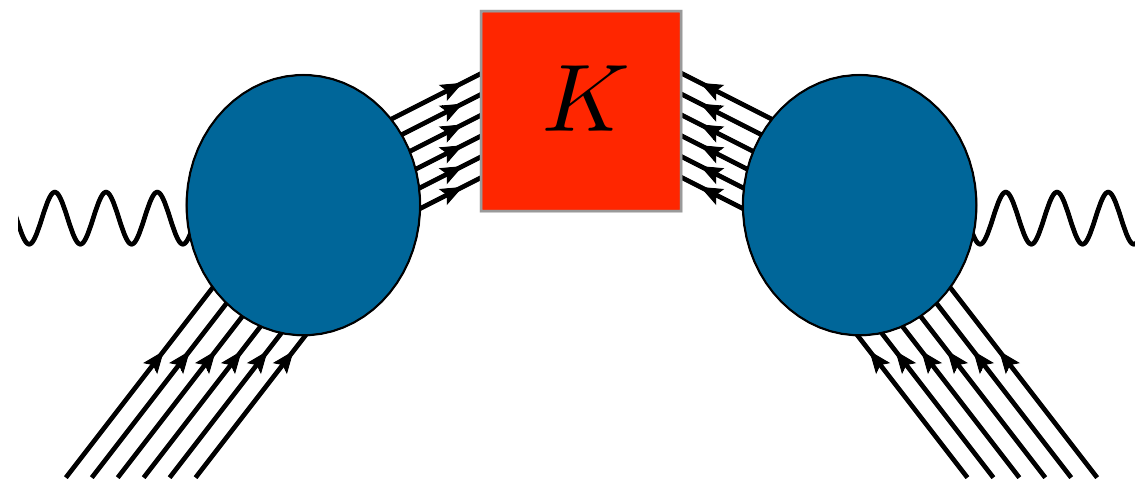
- The integral transform of the response function are generally defined as

$$E_{\alpha\beta}(\sigma, \mathbf{q}) \equiv \int d\omega K(\sigma, \omega) R_{\alpha\beta}(\omega, \mathbf{q})$$

$$R_{\alpha\beta}(\omega, \mathbf{q}) = \sum_f \langle \Psi_0 | J_\alpha^\dagger(\mathbf{q}) | \Psi_f \rangle \langle \Psi_f | J_\beta(\mathbf{q}) | \Psi_0 \rangle \delta(\omega - E_f + E_0)$$

- Using the completeness of the final states, they can be expressed in terms of ground-state expectation values

$$E_{\alpha\beta}(\sigma, \mathbf{q}) = \langle \Psi_0 | J_\alpha^\dagger(\mathbf{q}) K(\sigma, H - E_0) J_\beta(\mathbf{q}) | \Psi_0 \rangle$$



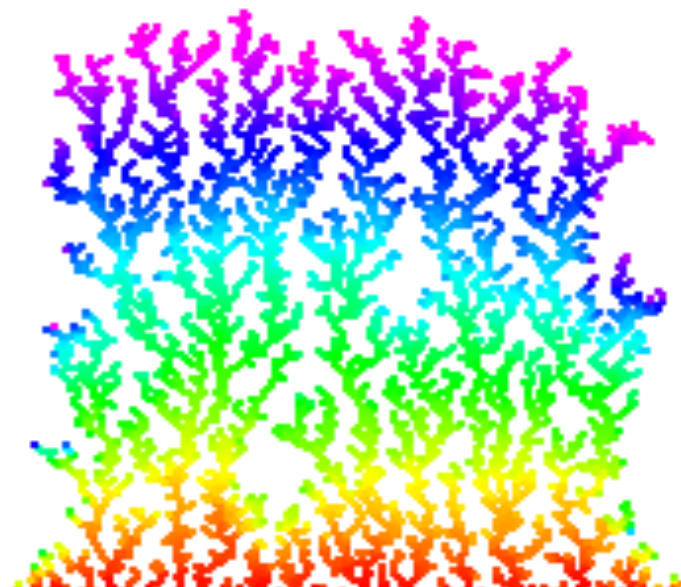
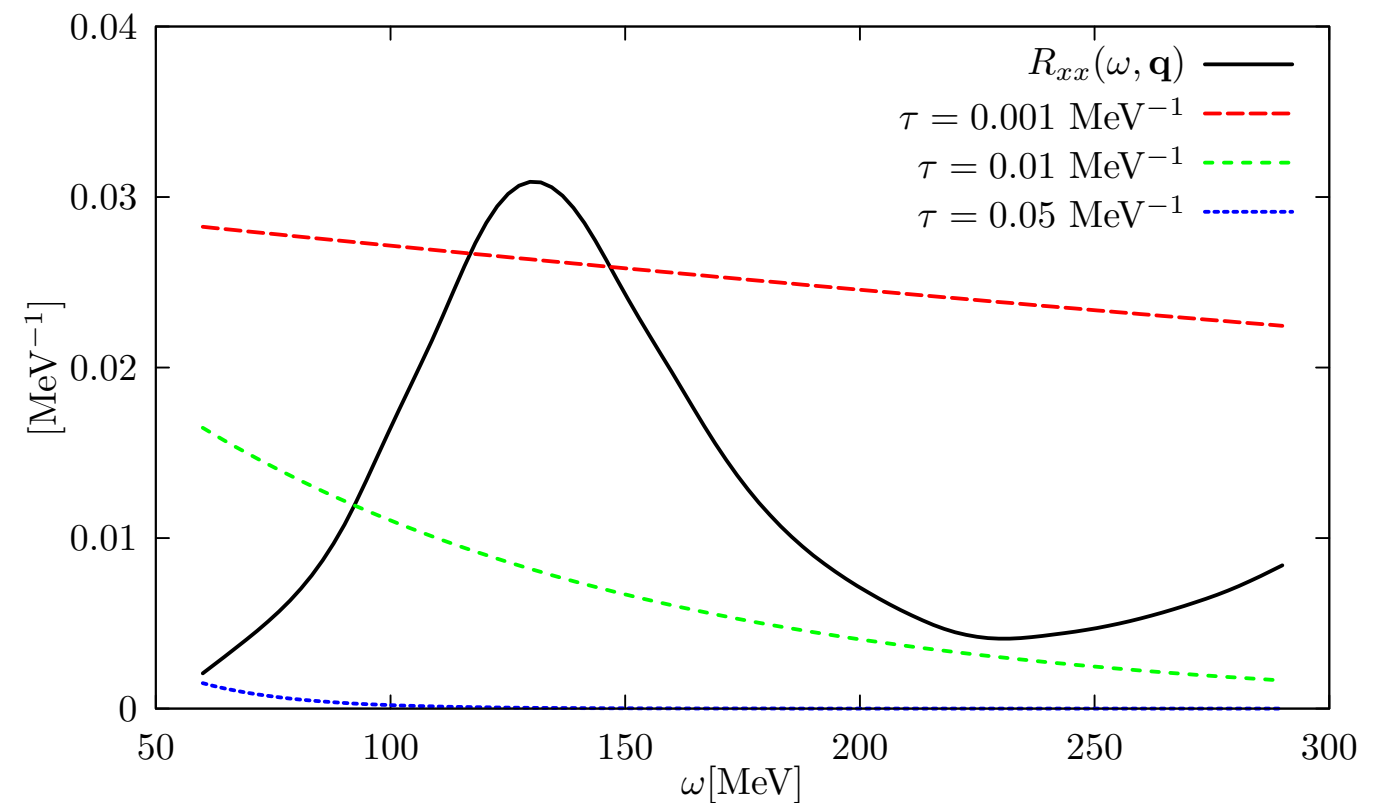
- Long- and short- range correlations are fully accounted for

Euclidean response function

Valuable information on the energy dependence of the response functions can be inferred from their Laplace transforms

$$E_{\alpha\beta}(\tau, \mathbf{q}) \equiv \int d\omega e^{-\omega\tau} R_{\alpha\beta}(\omega, \mathbf{q})$$

At finite imaginary time the contributions from large energy transfer are quickly suppressed



The system is first heated up by the transition operator. Its cooling determines the Euclidean response of the system

$$E_{\alpha\beta}(\tau, \mathbf{q}) = \langle \Psi_0 | J_{\alpha}^{\dagger}(\mathbf{q}) e^{-(H-E_0)\tau} J_{\beta}(\mathbf{q}) | \Psi_0 \rangle$$

Same technique used in Lattice QCD, condensed matter physics...

Euclidean response function

Inverting the Euclidean response is an ill posed problem: any set of observations is limited and noisy and the situation is even worse since the kernel is a smoothing operator.

$$E_{\alpha\beta}(\tau, \mathbf{q}) \longrightarrow R_{\alpha\beta}(\omega, \mathbf{q})$$



Image reconstruction from incomplete and noisy data

S. F. Gull & G. J. Daniell*

Mullard Radio Astronomy Observatory, Cavendish Laboratory, Madingley Road, Cambridge, UK

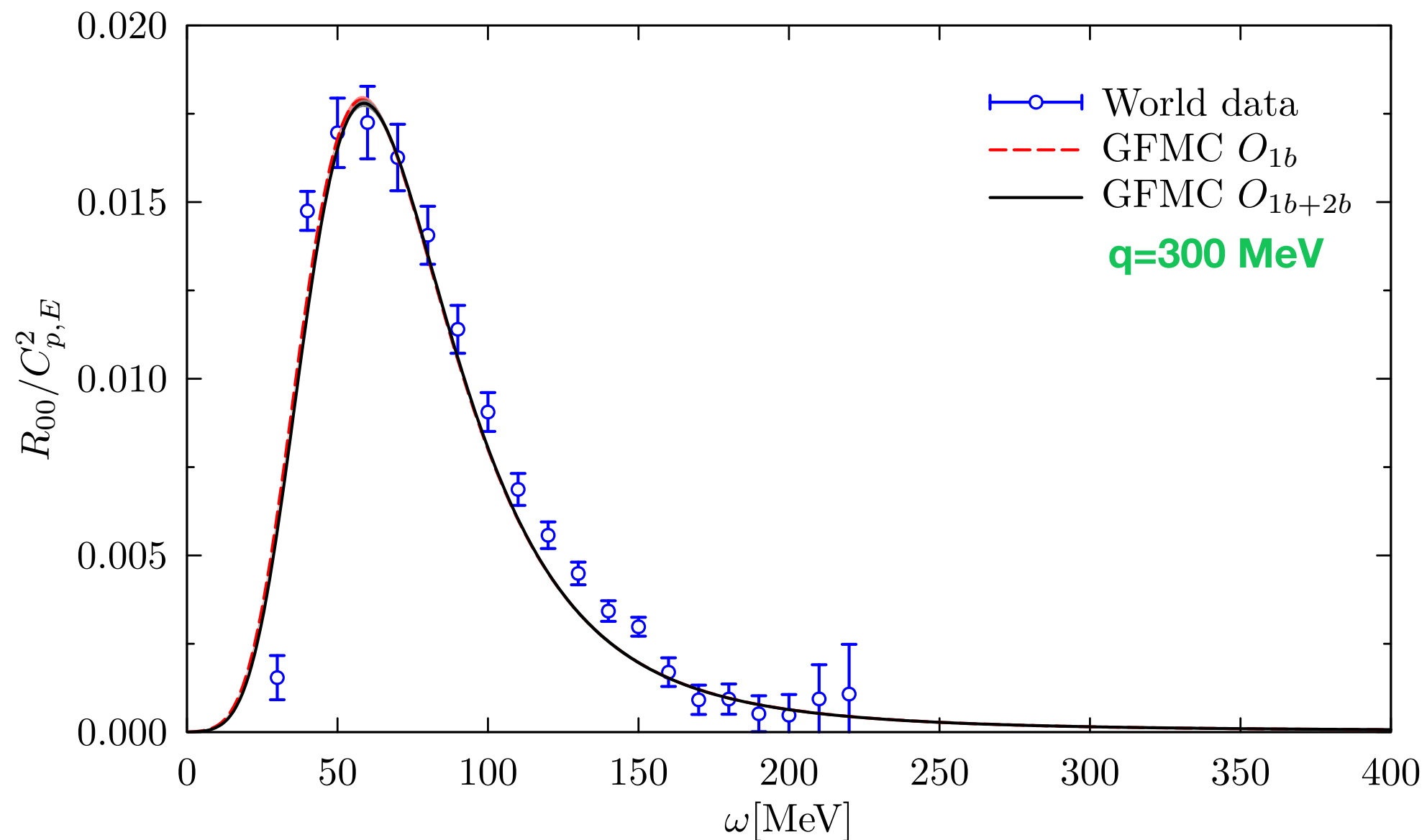
Results are presented of a powerful technique for image reconstruction by a maximum entropy method, which is sufficiently fast to be useful for large and complicated images. Although our examples are taken from the fields of radio and X-ray astronomy, the technique is immediately applicable in spectroscopy, electron microscopy, X-ray crystallography, geophysics and virtually any type of optical image processing. Applied to radioastronomical data, the algorithm reveals details not seen by conventional analysis, but which are known to exist.

To avoid abstraction, we shall refer to our radioastronomical example. Starting with incomplete and noisy data, one can obtain by the Backus–Gilbert method a series of maps of the distribution of radio brightness across the sky, all of which are consistent with the data, but have different resolutions and noise levels. From the data alone, there is no reason to prefer any one of these maps, and the observer may select the most appropriate one to answer any specific question. Hence, the method cannot produce a unique ‘best’ map of the sky. There is no single map that is equally suitable for discussing both accurate flux measurements and source positions.

Nevertheless, it is useful to have a single general-purpose map of the sky, and the maximum-entropy map described here fulfils

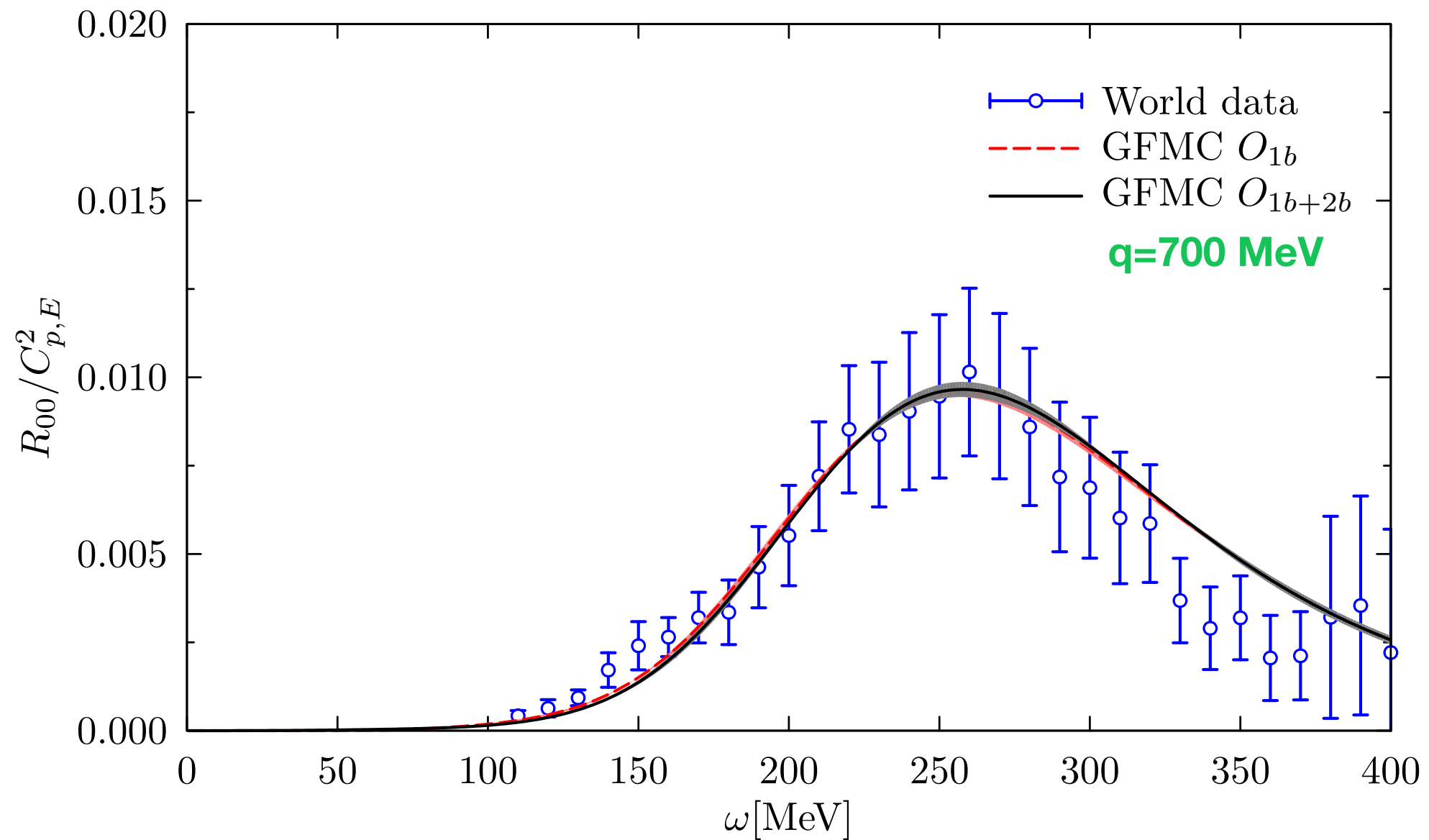
^4He electromagnetic response

Two-body currents do not provide significant changes in the longitudinal response.
The agreement with experimental data appears to be remarkably good.



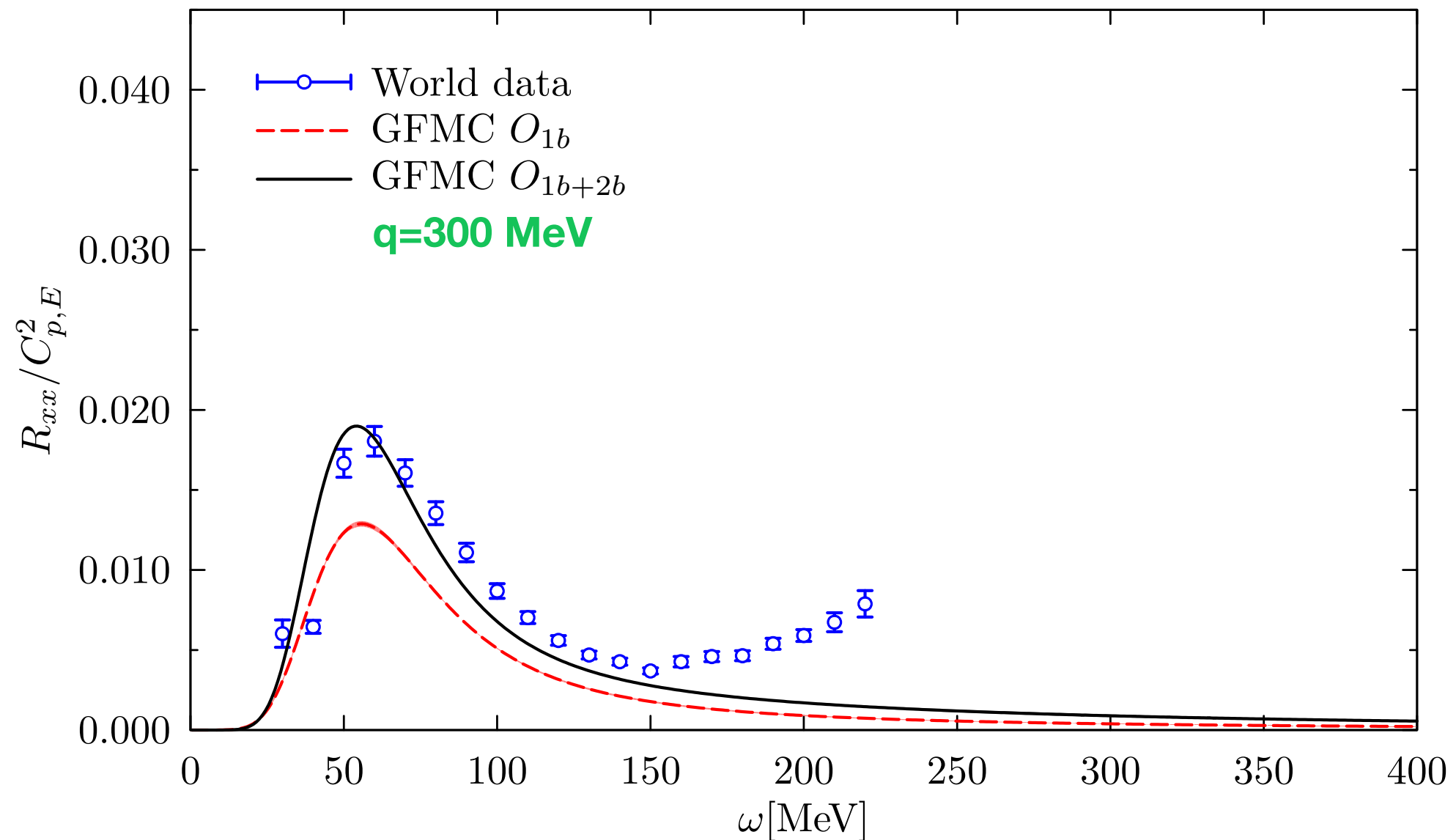
^4He electromagnetic response

Two-body currents do not provide significant changes in the longitudinal response.
The agreement with experimental data appears to be remarkably good.



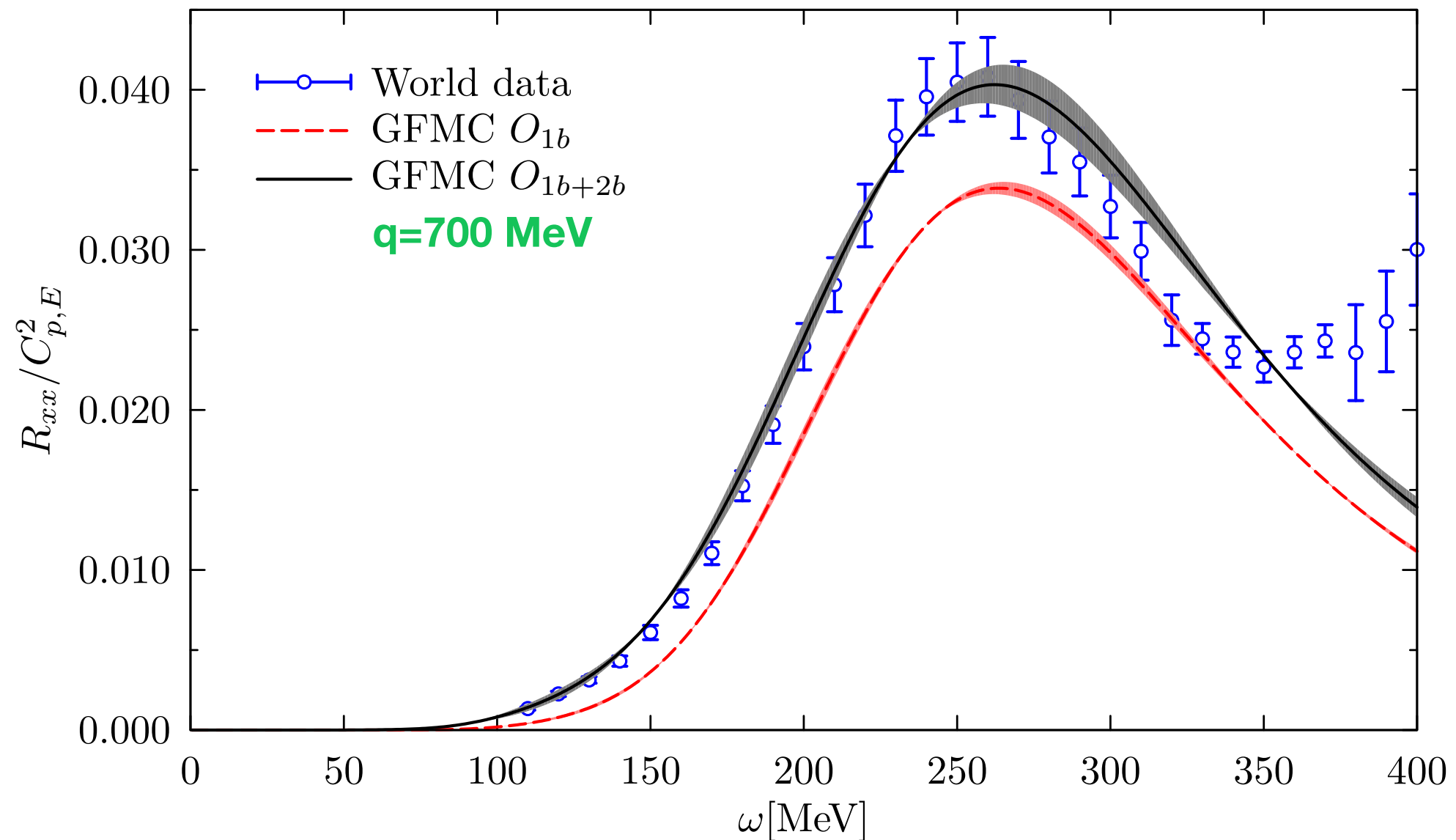
^4He electromagnetic response

Two-body currents significantly enhance the transverse response function, not only in the dip region, but also in the quasielastic peak and threshold regions. They are needed for a better agreement with the experimental data.



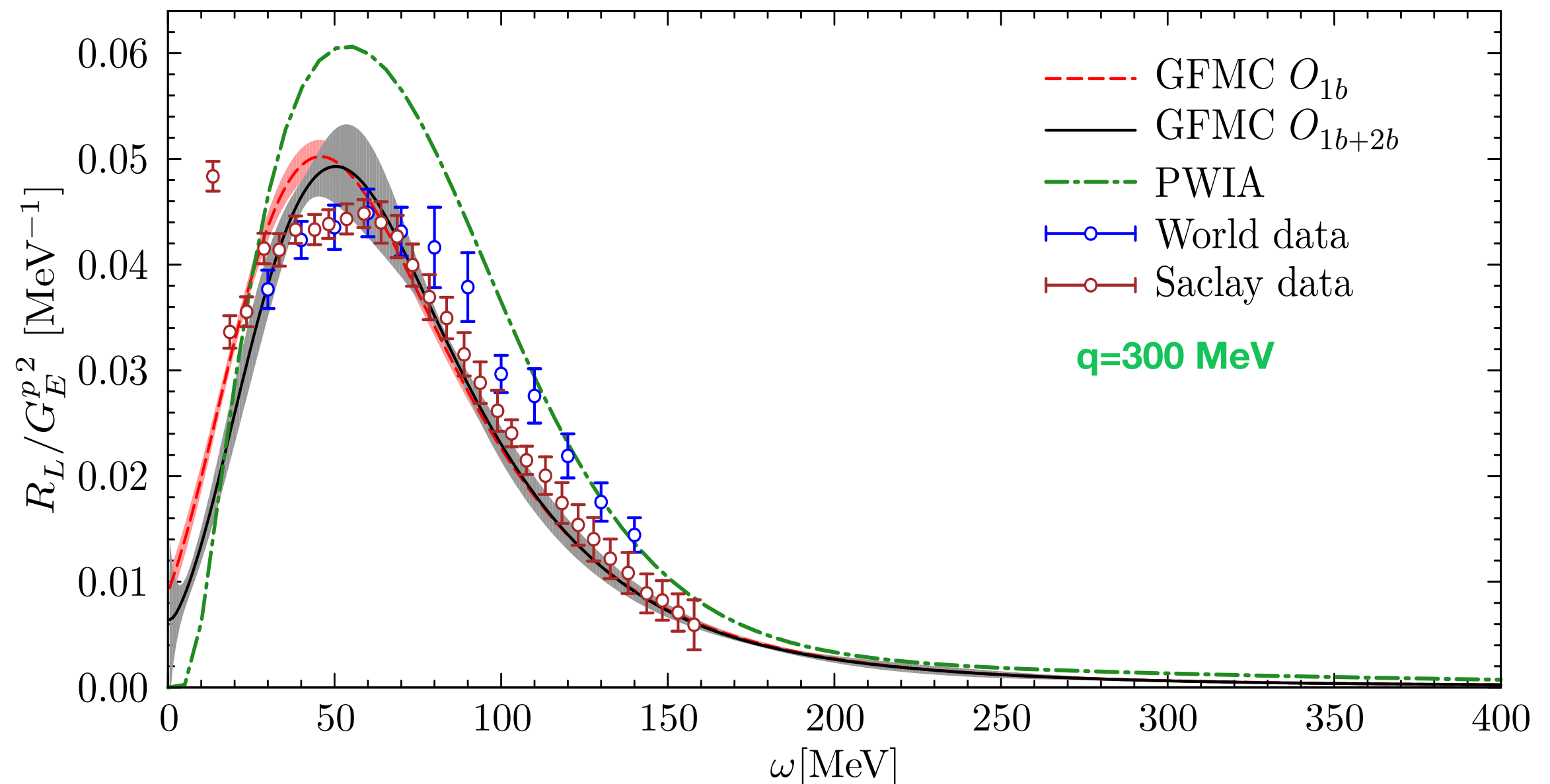
^4He electromagnetic response

Two-body currents significantly enhance the transverse response function, not only in the dip region, but also in the quasielastic peak and threshold regions. They are needed for a better agreement with the experimental data



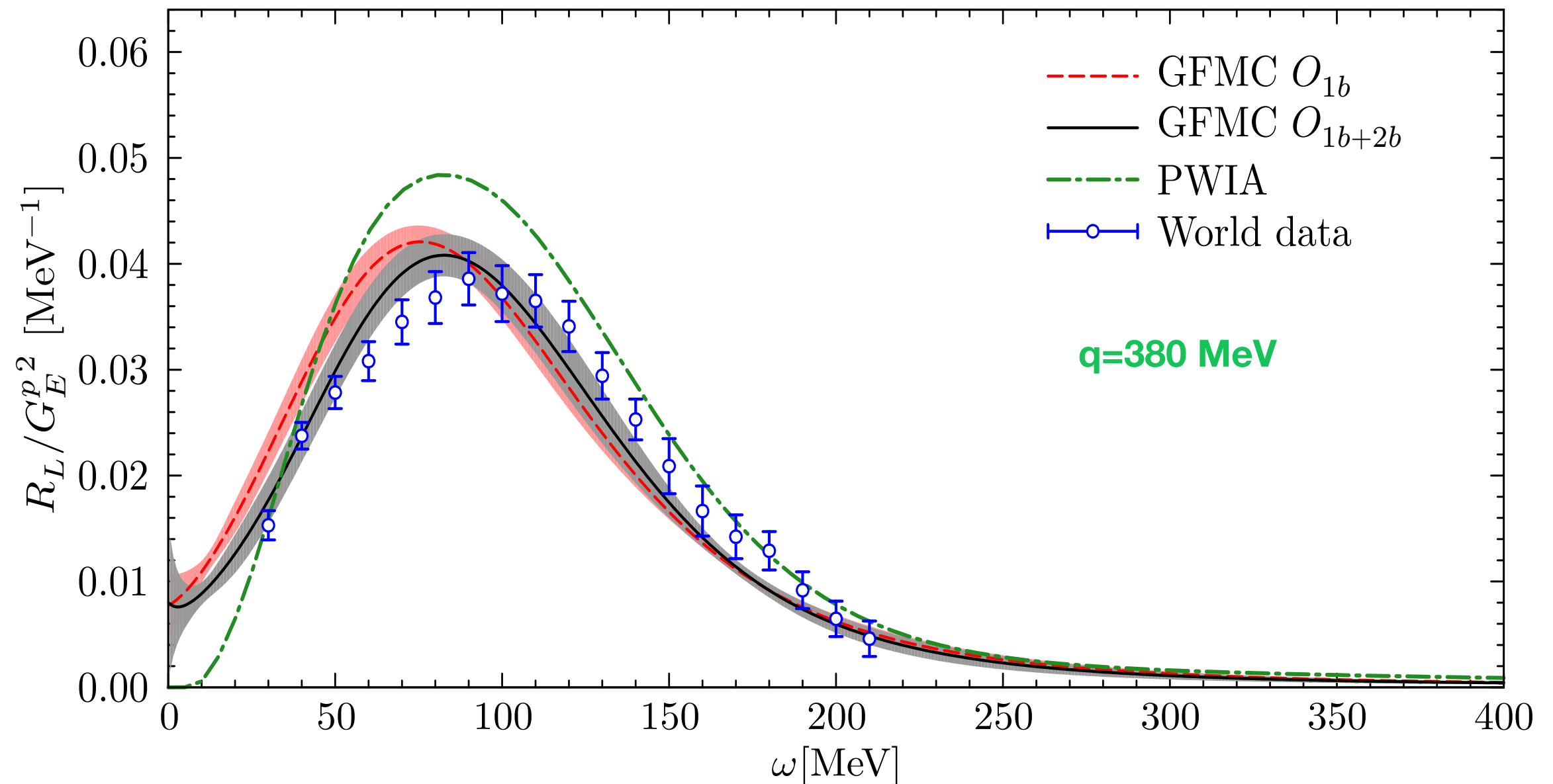
^{12}C electromagnetic response

- We were recently able to invert the electromagnetic Euclidean response of ^{12}C :
first ab-initio calculation of the electromagnetic response of ^{12}C !
- Very good agreement with the experimental data. Small contribution from two-body currents.



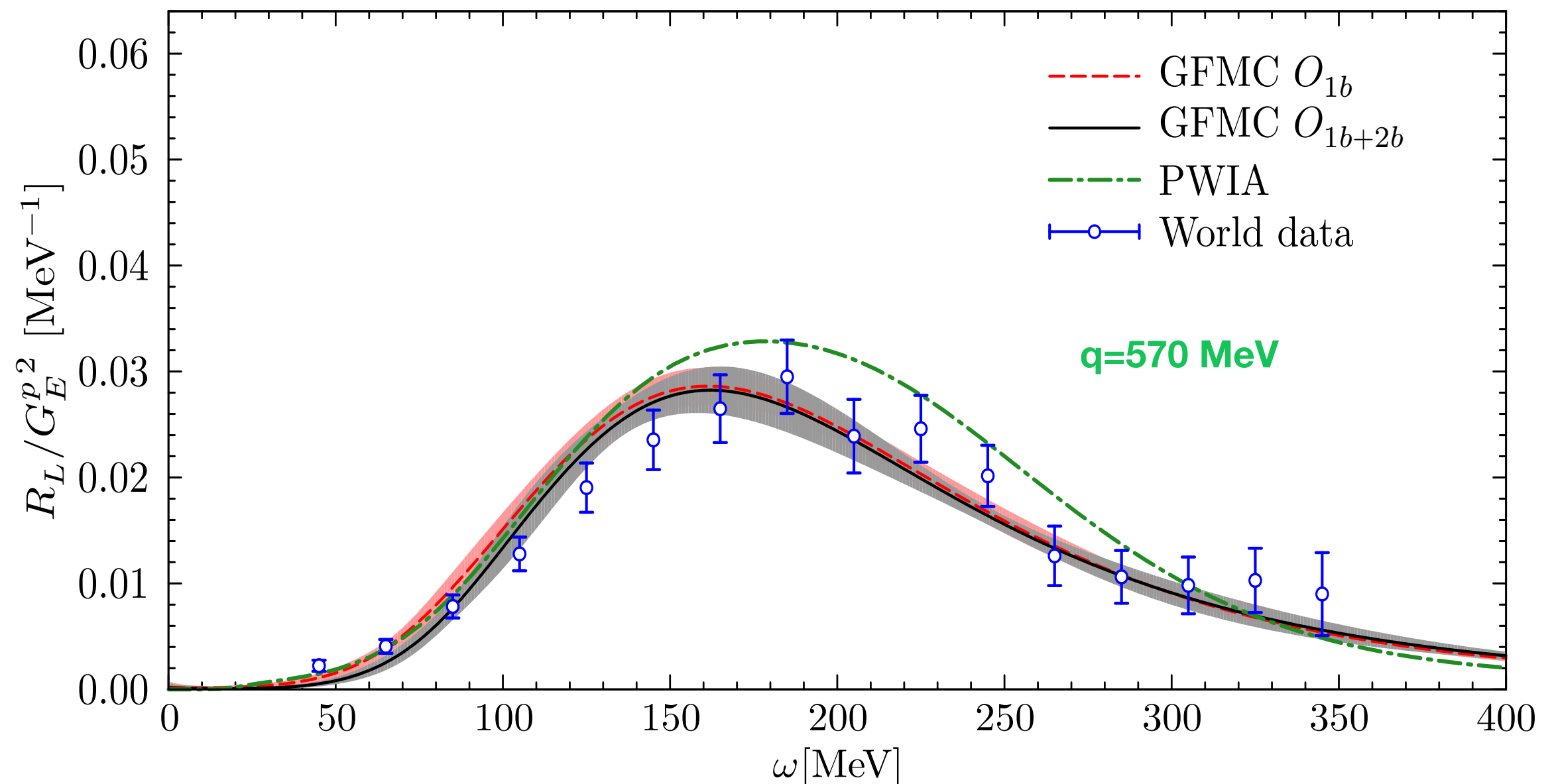
^{12}C electromagnetic response

- We were recently able to invert the electromagnetic Euclidean response of ^{12}C :
first ab-initio calculation of the electromagnetic response of ^{12}C !
- Very good agreement with the experimental data. Small contribution from two-body currents.



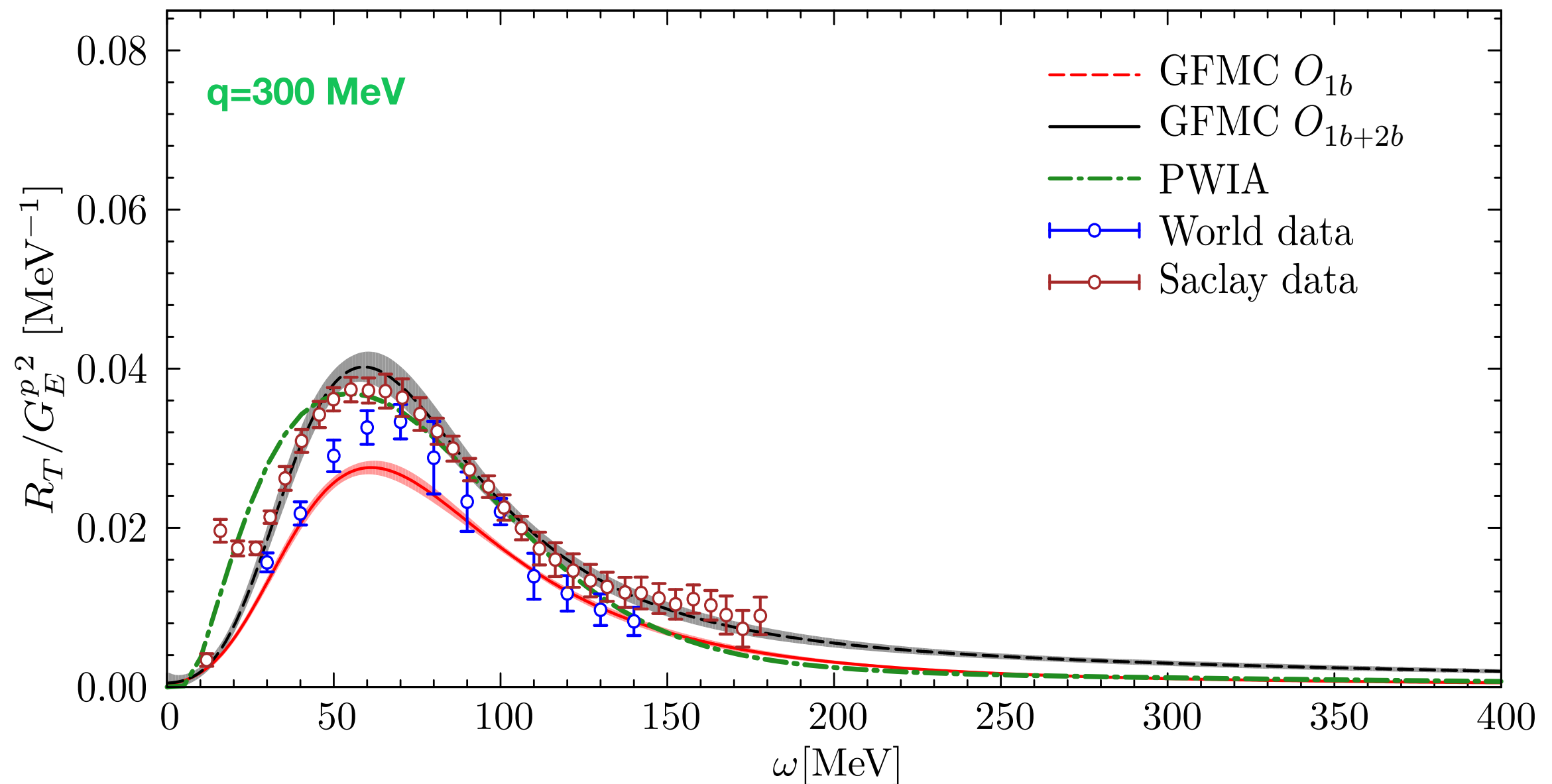
^{12}C electromagnetic response

- We were recently able to invert the electromagnetic Euclidean response of ^{12}C :
first ab-initio calculation of the electromagnetic response of ^{12}C !
- Very good agreement with the experimental data. Small contribution from two-body currents.



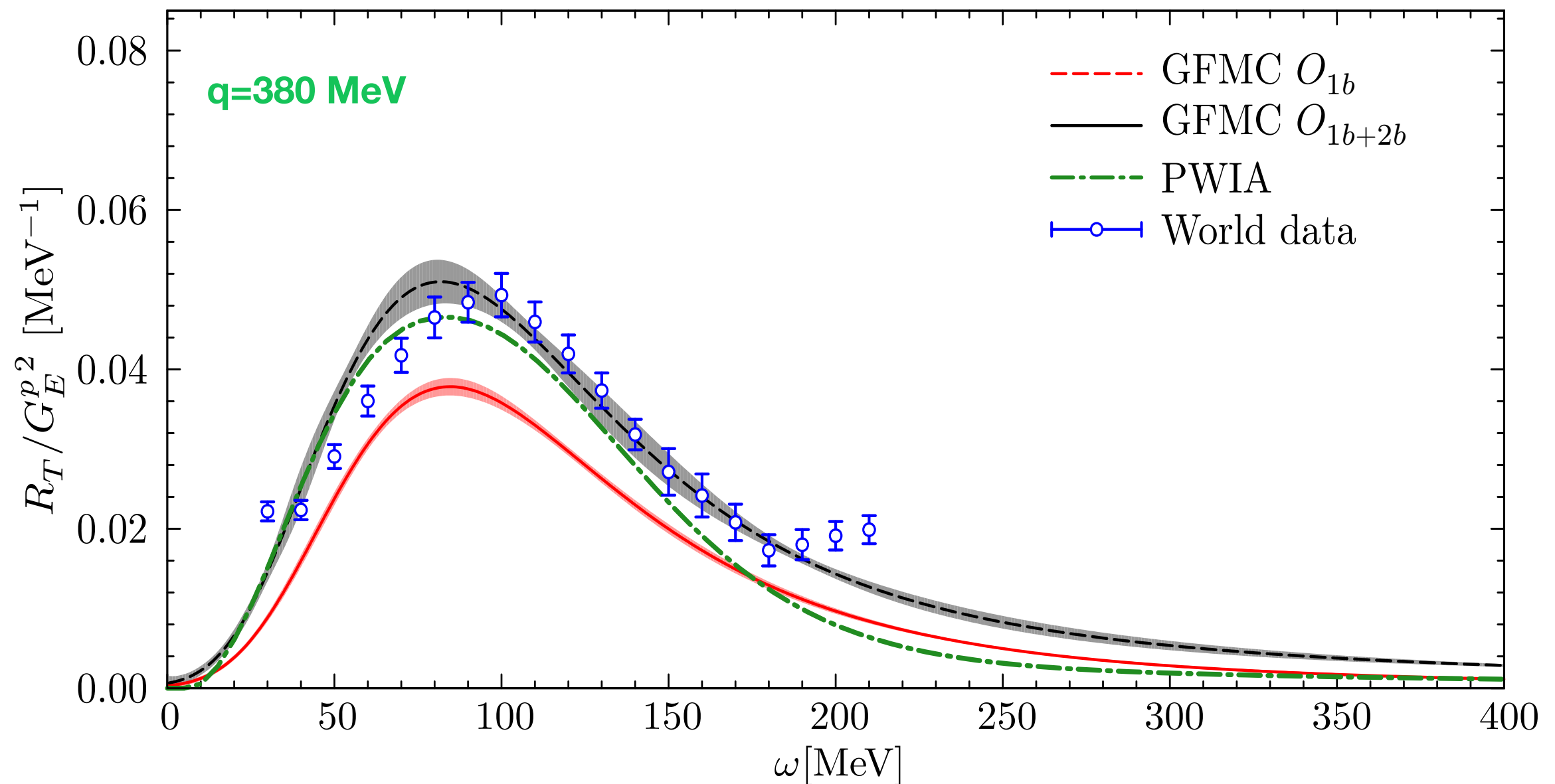
^{12}C electromagnetic response

- We were recently able to invert the electromagnetic Euclidean response of ^{12}C :
first ab-initio calculation of the electromagnetic response of ^{12}C !
- Very good agreement with the experimental data once two-body currents are accounted for!



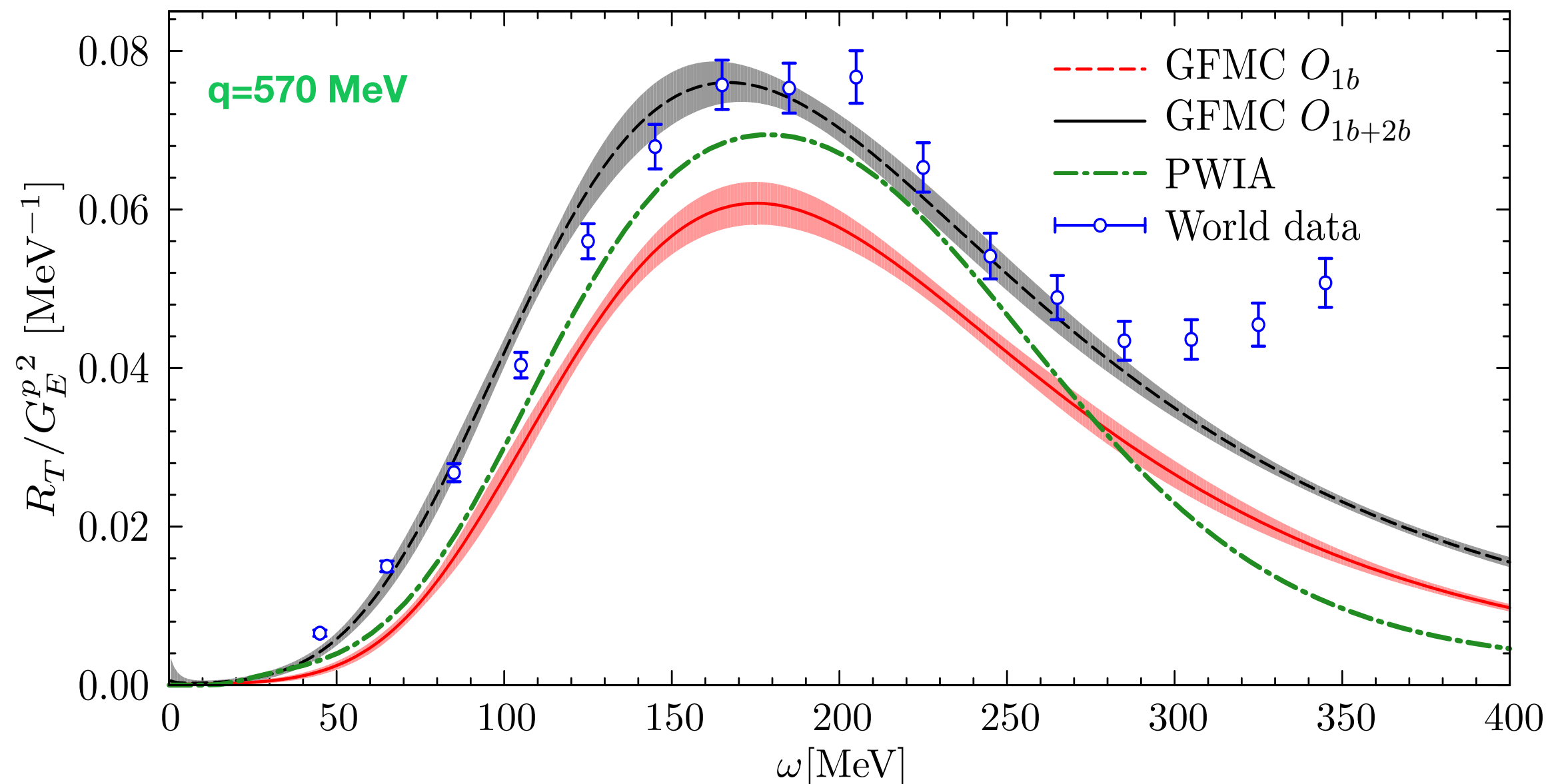
^{12}C electromagnetic response

- We were recently able to invert the electromagnetic Euclidean response of ^{12}C :
first ab-initio calculation of the electromagnetic response of ^{12}C !
- Very good agreement with the experimental data once two-body currents are accounted for!



^{12}C electromagnetic response

- We were recently able to invert the electromagnetic Euclidean response of ^{12}C :
first ab-initio calculation of the electromagnetic response of ^{12}C !
- Very good agreement with the experimental data once two-body currents are accounted for!



Transverse enhancement

- The enhancement in the quasi elastic peak is surprising, but NOT NEW

PHYSICAL REVIEW C

VOLUME 55, NUMBER 1

JANUARY 1997

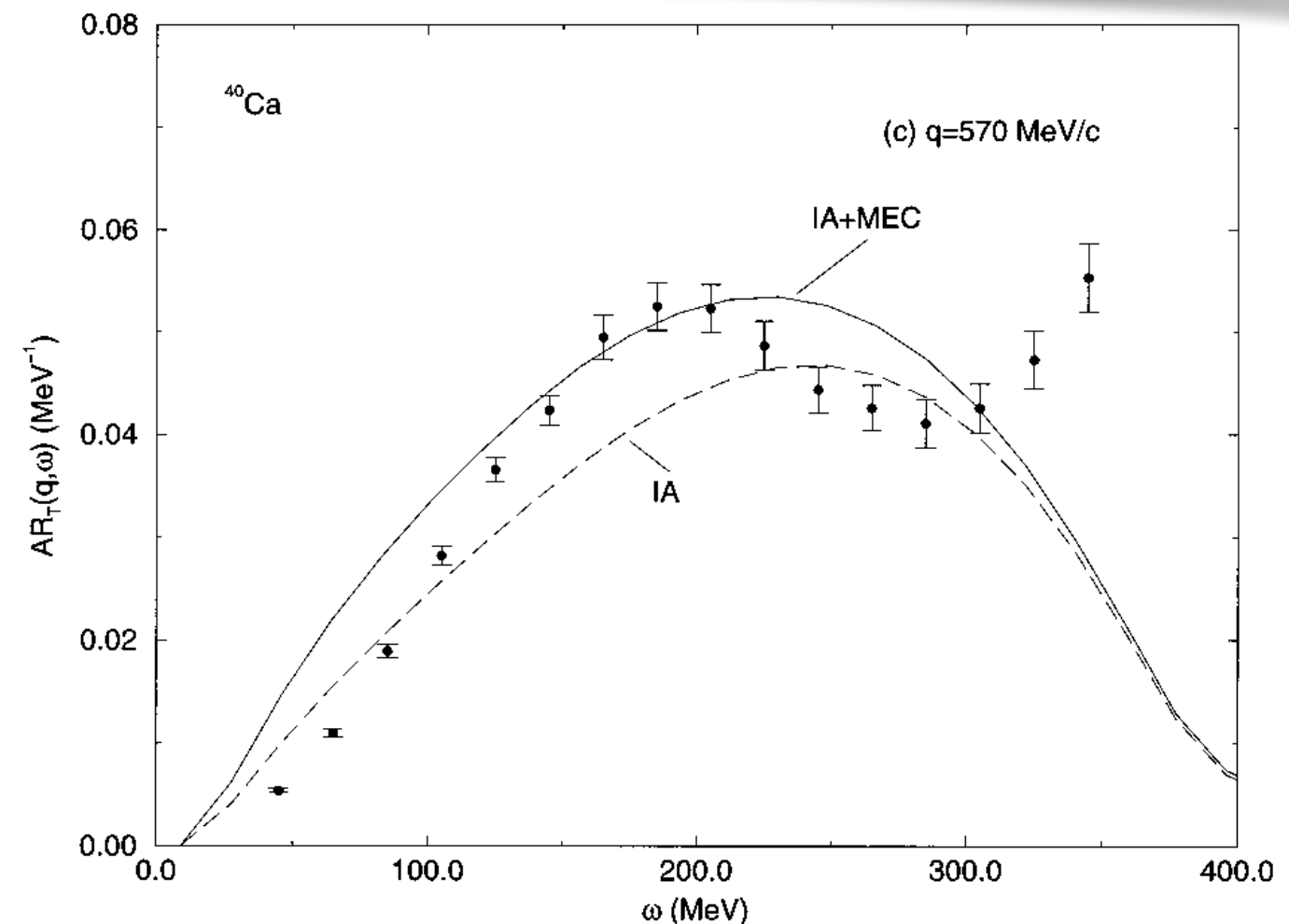
Inclusive transverse response of nuclear matter

Adelchi Fabrocini

- Back in 1997 Adelchi Fabrocini found a significant enhancement of the transverse response function from two-body current

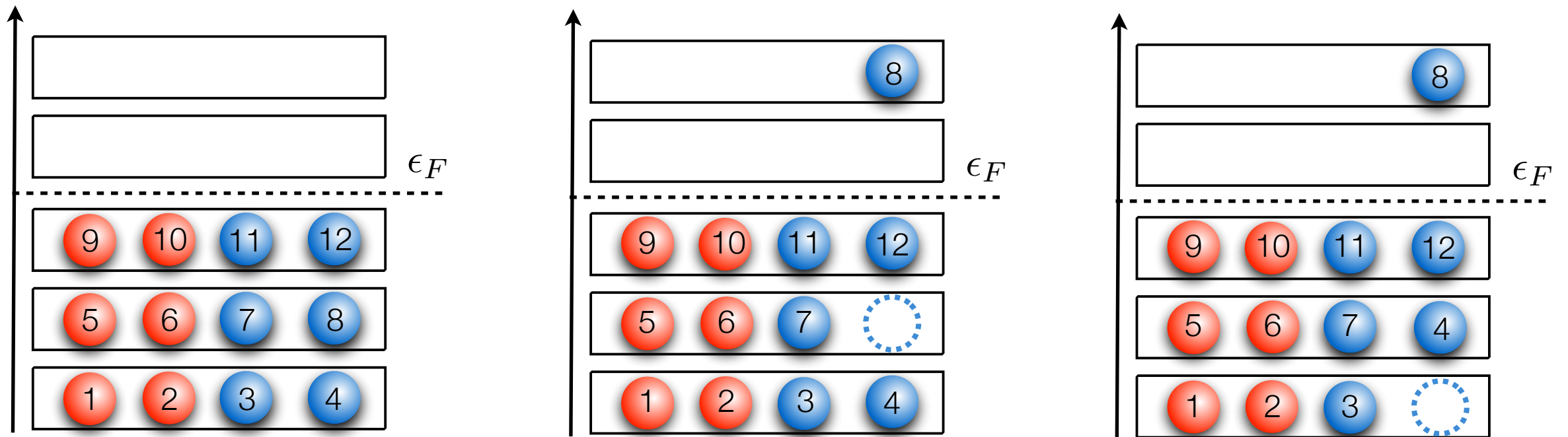
- This enhancement, in the quasielastic peak region, is due to one-particle one-hole final state

$$R_T^{1p1h}(q, \omega) = \frac{1}{A} \sum_{ph} |\langle 0 | \mathbf{j}(\mathbf{q}) | \mathbf{ph} \rangle|^2 \delta(\omega - e_p + e_h)$$



Transverse enhancement

- Two-body currents can give rise to one-particle one-hole final states



- Such processes also occur in a mean-field picture of the nucleus
- This effect is potentially large in the quasi elastic peak.
- Two-body currents contribute to the $e(e' p)$ cross section

Open remarks

- One-particle one-hole, two-particle two-hole states are definition dependent

- * In infinite nuclear matter single particle orbitals are plane waves

- * In atomic nuclei they are given by solving the Hartree-Fock equations associated with the mean field potential

$$\left[\sum_{i < j} v_{ij} + \sum_{i < j < k} V_{ijk} \right] \rightarrow \sum_i U_i$$

- * Differences between correlated (Omar, Noemi...) and uncorrelated (Juan, Marco, Bill...) states

$$\Phi_{p_i, h_i}(x_1 \dots x_A) = \mathcal{A}[\phi_{n_1}(x_1) \dots \phi_{p_i}(x_i) \dots \phi_{n_A}(x_A)]$$

$$\Psi_{p_i, h_i}(x_1 \dots x_A) = \mathcal{F}\mathcal{A}[\phi_{n_1}(x_1) \dots \phi_{p_i}(x_i) \dots \phi_{n_A}(x_A)]$$

- * Correlated n-particle n-holes correlated states are closer to the eigenstates of the nuclear Hamiltonian

- * RPA can be much larger in uncorrelated many-body states than in correlated ones

Large momentum transfer

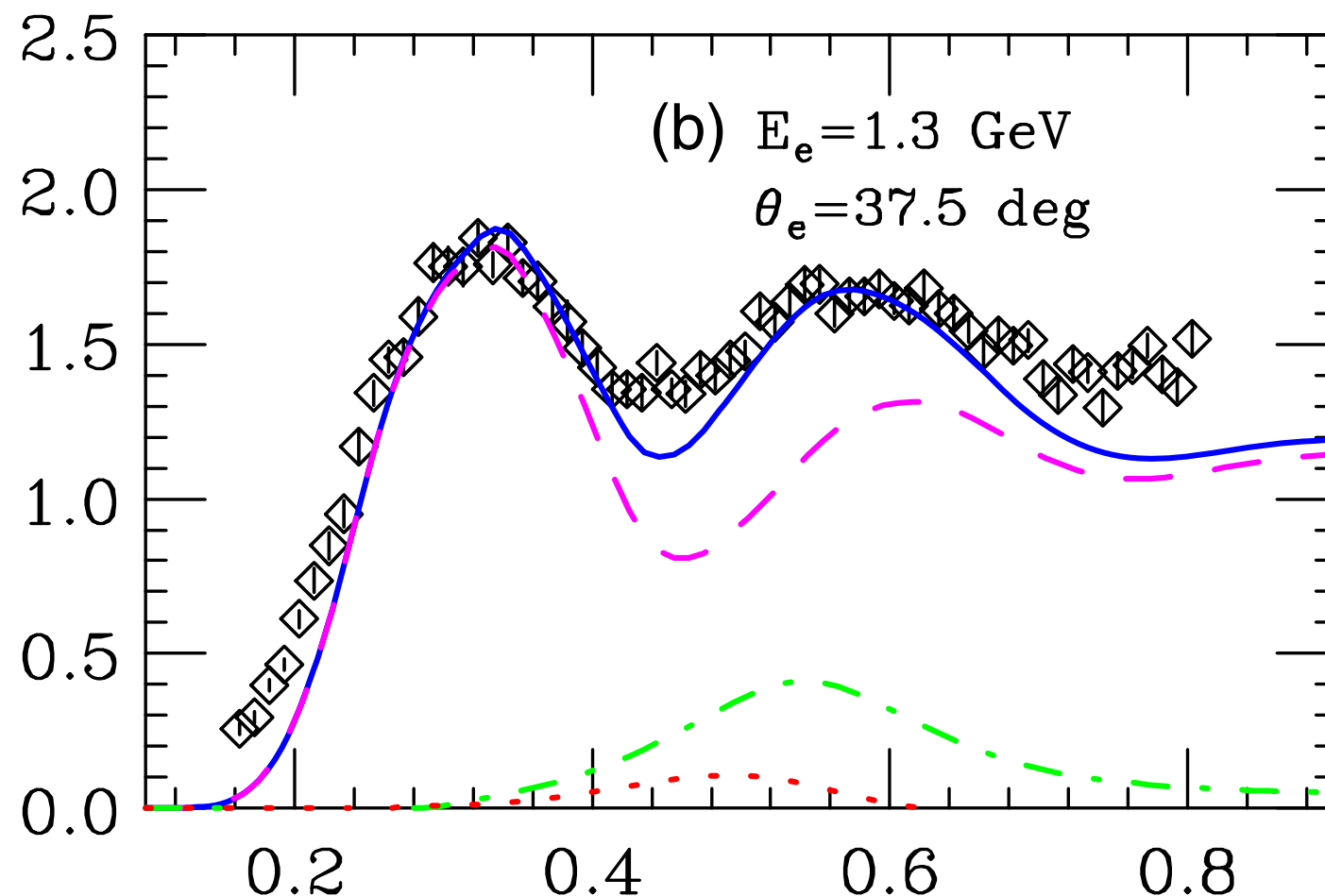
Spectral function approach

To use relativistic MEC and realistic description of the nuclear ground state, we have extended the factorization scheme to account for two-nucleon emission amplitude

$$|\Psi_f\rangle \rightarrow |\mathbf{p}\rangle \otimes |\Psi_{\tilde{f}}\rangle_{A-1}$$

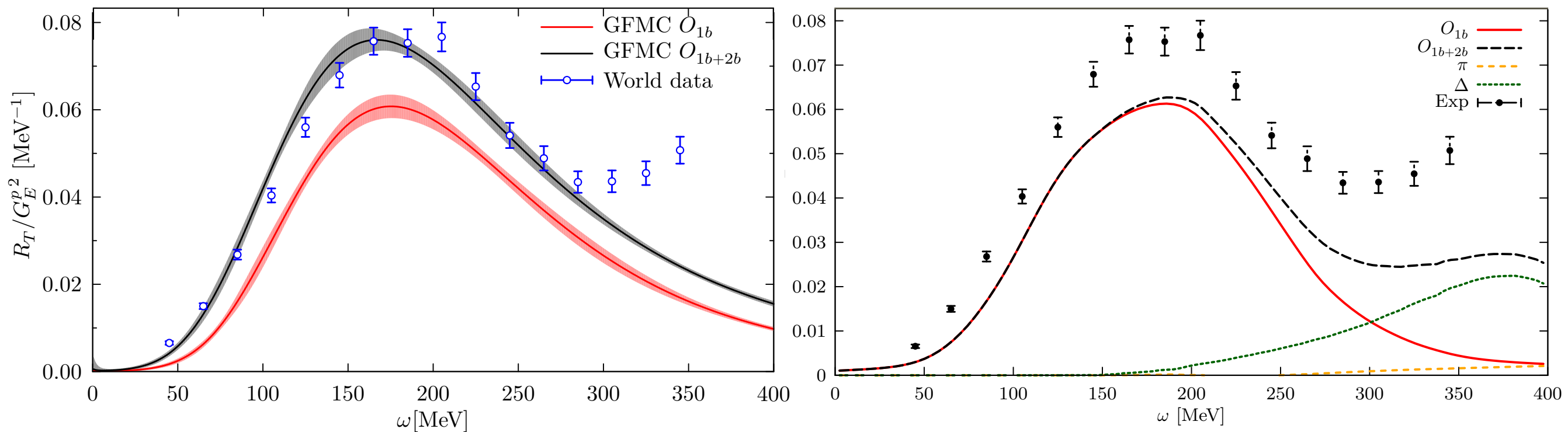
$$|\Psi_f\rangle \rightarrow |\mathbf{pp}'\rangle \otimes |\Psi_{\tilde{f}}\rangle_{A-2}$$

We computed the inclusive electromagnetic cross section of ^{12}C . The effect of relativistic two-body currents is sizable in the dip region



Spectral function vs GFMC

We have some problems here



This discrepancy can be ascribed to

- Differences in the two-nucleon currents employed in the two cases
- The non relativistic nature of the GFMC calculations
- Interference between amplitudes involving the one- and two-body currents and 1p1h final states

Spectral function vs GFMC

- We started comparing the one-body results

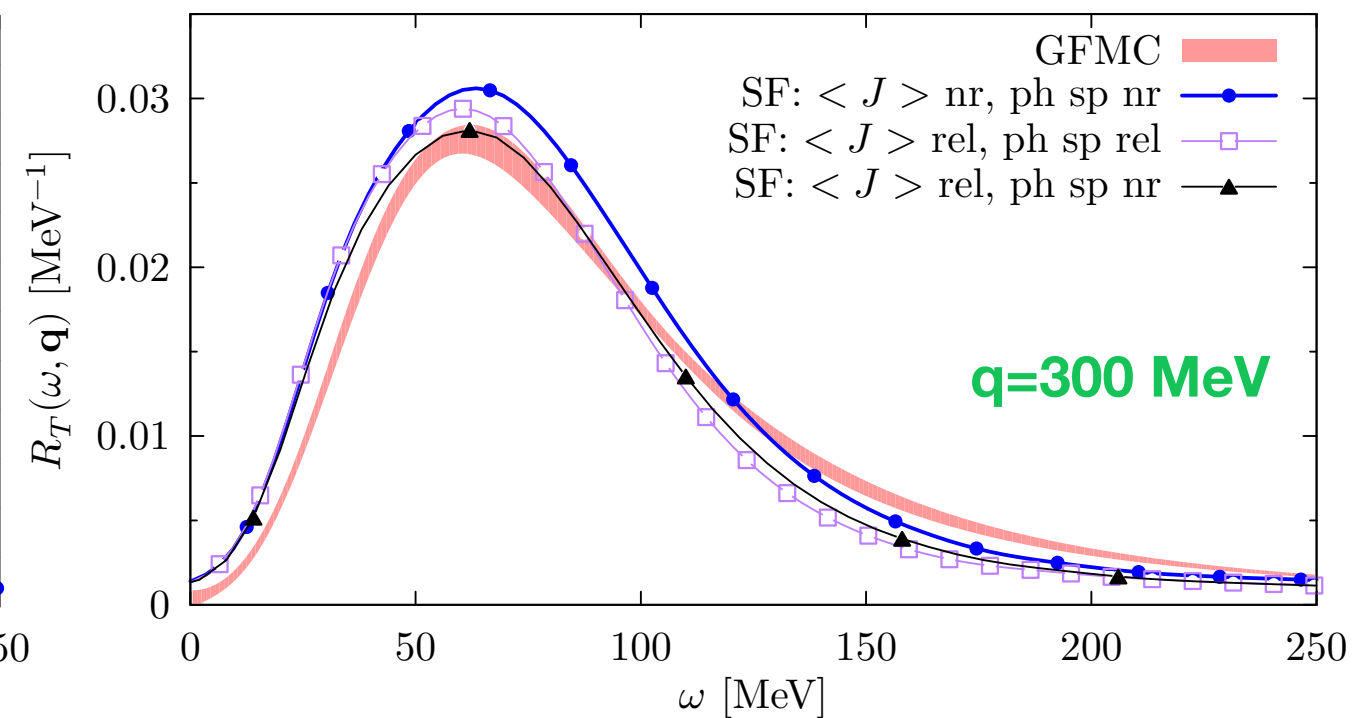
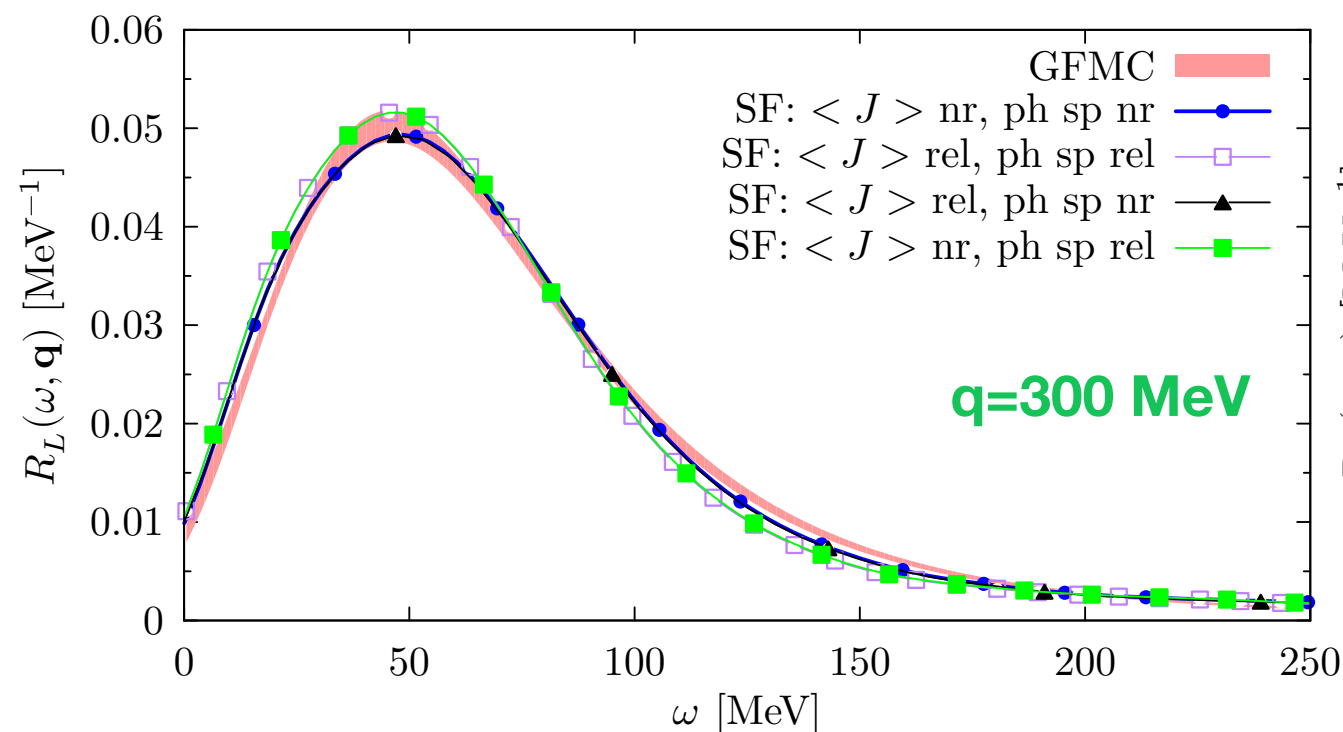
$$R^{\alpha\beta} = \int dE d\mathbf{p} P(\mathbf{p}, E) \sum_i \langle p | j_i^{\alpha\dagger} | p + q \rangle \langle p + q | j_i^\beta | p \rangle \frac{m^2}{E_p E_{p+q}} \delta[\omega + M_A - E_R - E_{p+q}]$$

- Relativity enters in the current matrix element and in the phase space

* In the GFMC a systematic expansion of the relativistic corrections is performed

* Relativistic effects are “maximum” in the impulse approximation

- The impulse approximation appears to be more reliable in the longitudinal than in the transverse channel

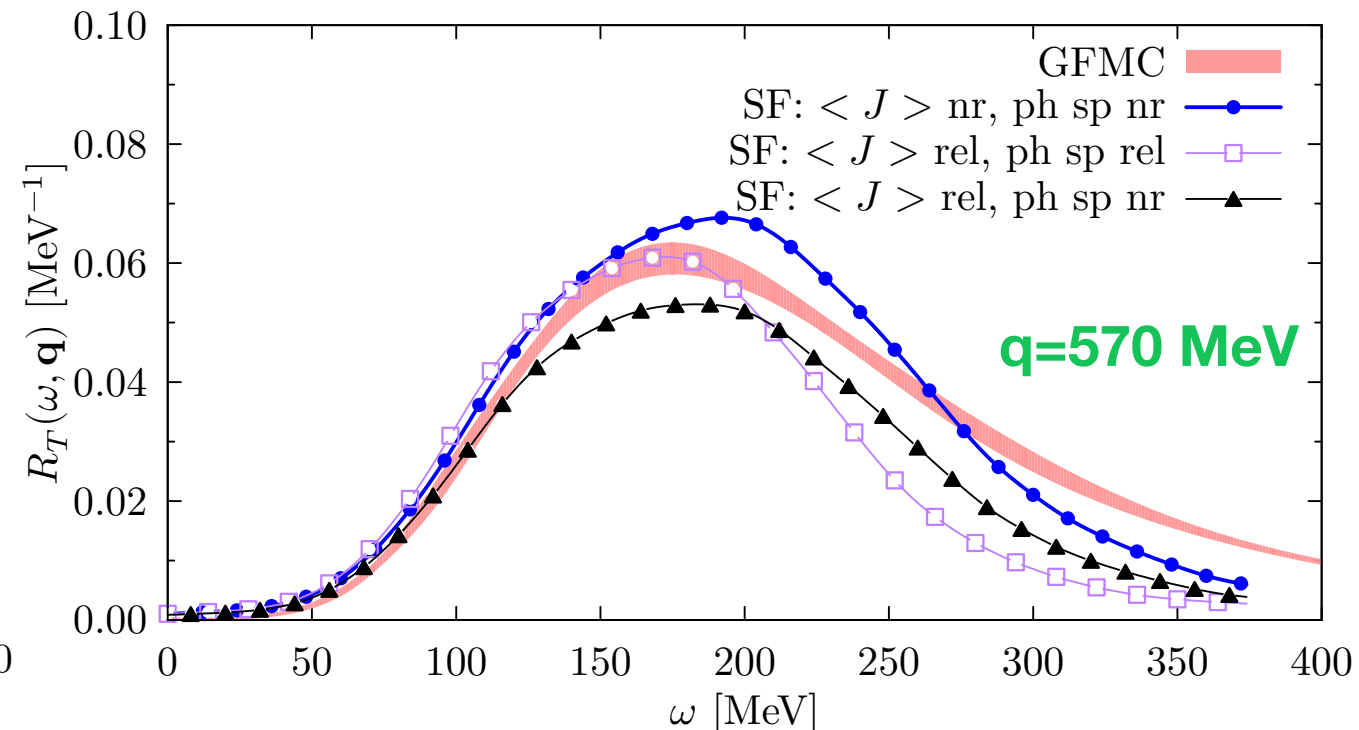
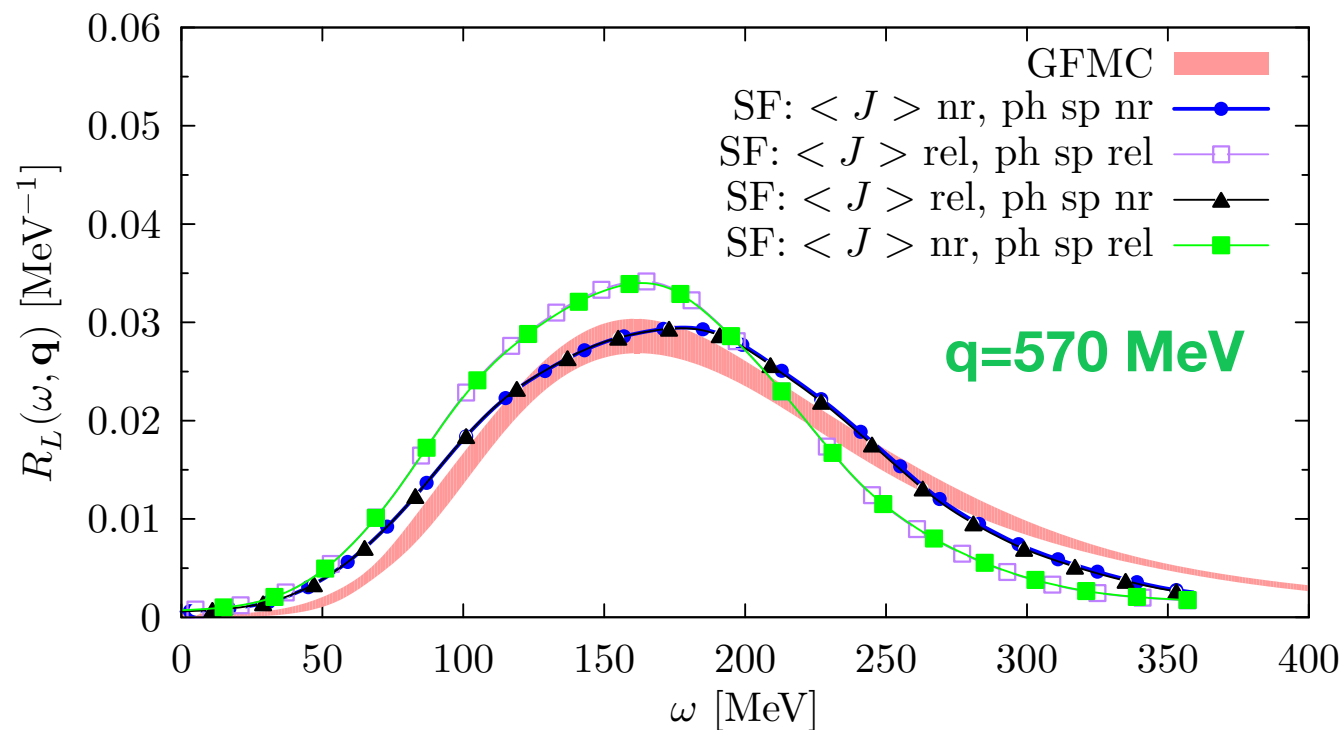


Spectral function vs GFMC

- We started comparing the one-body results

$$R^{\alpha\beta} = \int dE d\mathbf{p} P(\mathbf{p}, E) \sum_i \langle p | j_i^{\alpha\dagger} | p + q \rangle \langle p + q | j_i^\beta | p \rangle \frac{m^2}{E_p E_{p+q}} \delta[\omega + M_A - E_R - E_{p+q}]$$

- Relativity enters in the current matrix element and in the phase space
 - * In the GFMC a systematic expansion of the relativistic corrections is performed
 - * Relativistic effects are “maximum” in the impulse approximation
- Sizable relativistic effects in the phase space
- The transverse response is strongly affected by relativistic effects in the current operator

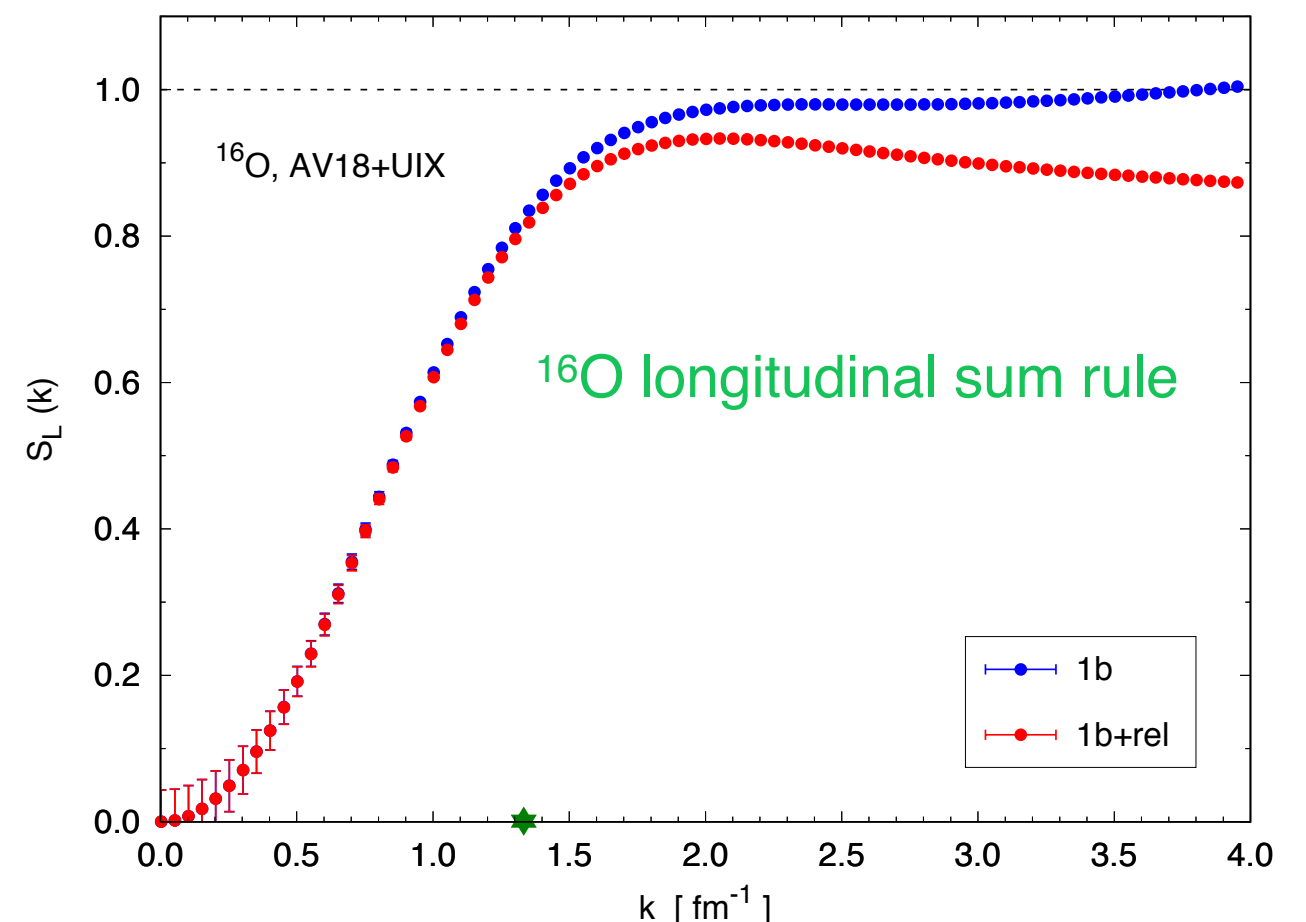
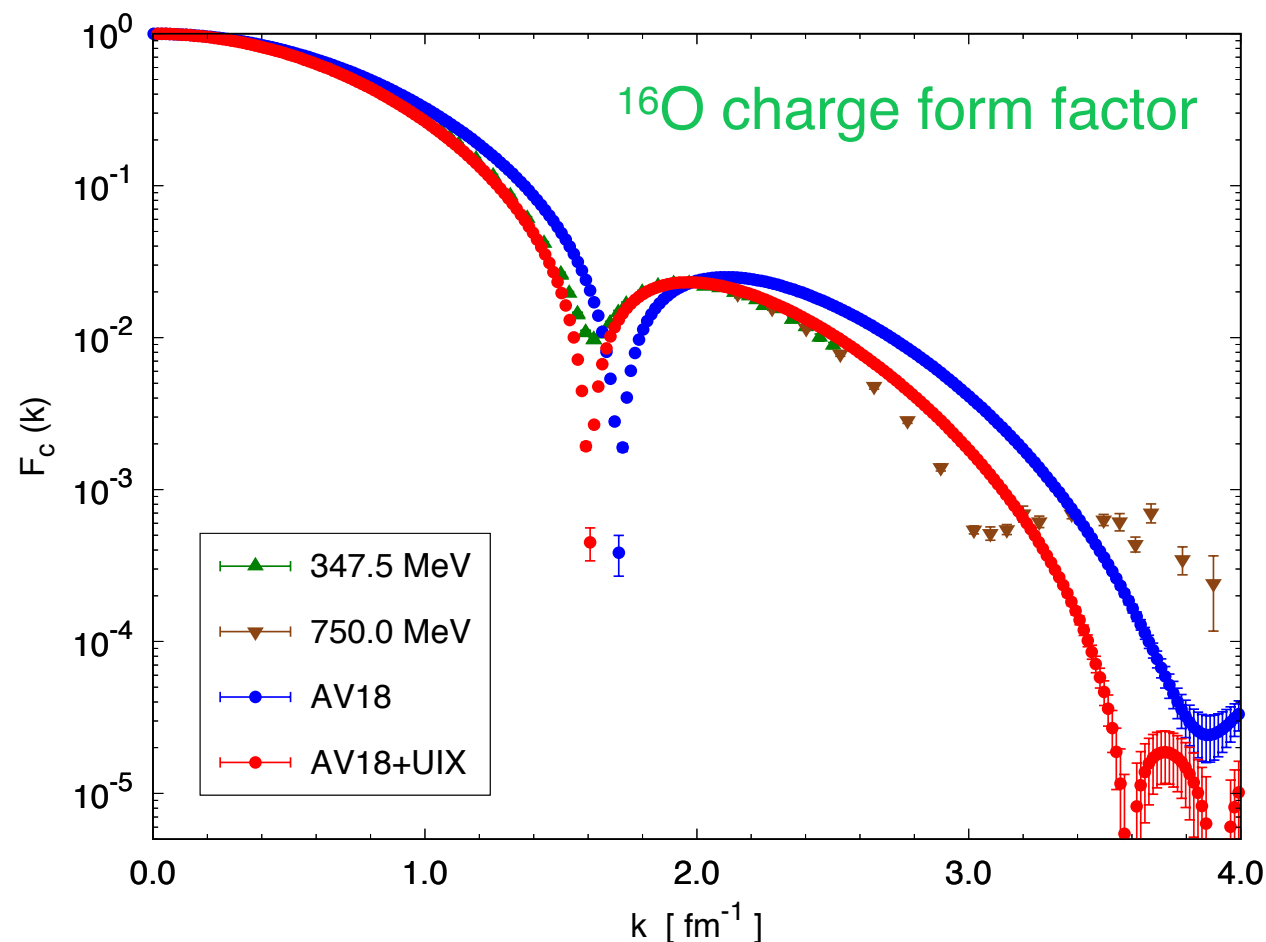


Larger nuclei: ^{16}O and ^{40}Ca

- In an effort led by Diego Lonardonì we are moving towards larger nuclei, like ^{16}O and ^{40}Ca
- Expectation values are evaluated using up to five-body clusters for the non-central correlations.

$$E_T = \sum_i c_i + \sum_{i<j} c_{ij} + \sum_{i<j<k} c_{ijk} + \sum_{i<j<k<l} c_{ijkl}$$

- We have computed the charge form factor (the axial one is relevant for dark matter detection) and the sum rules of the longitudinal response functions



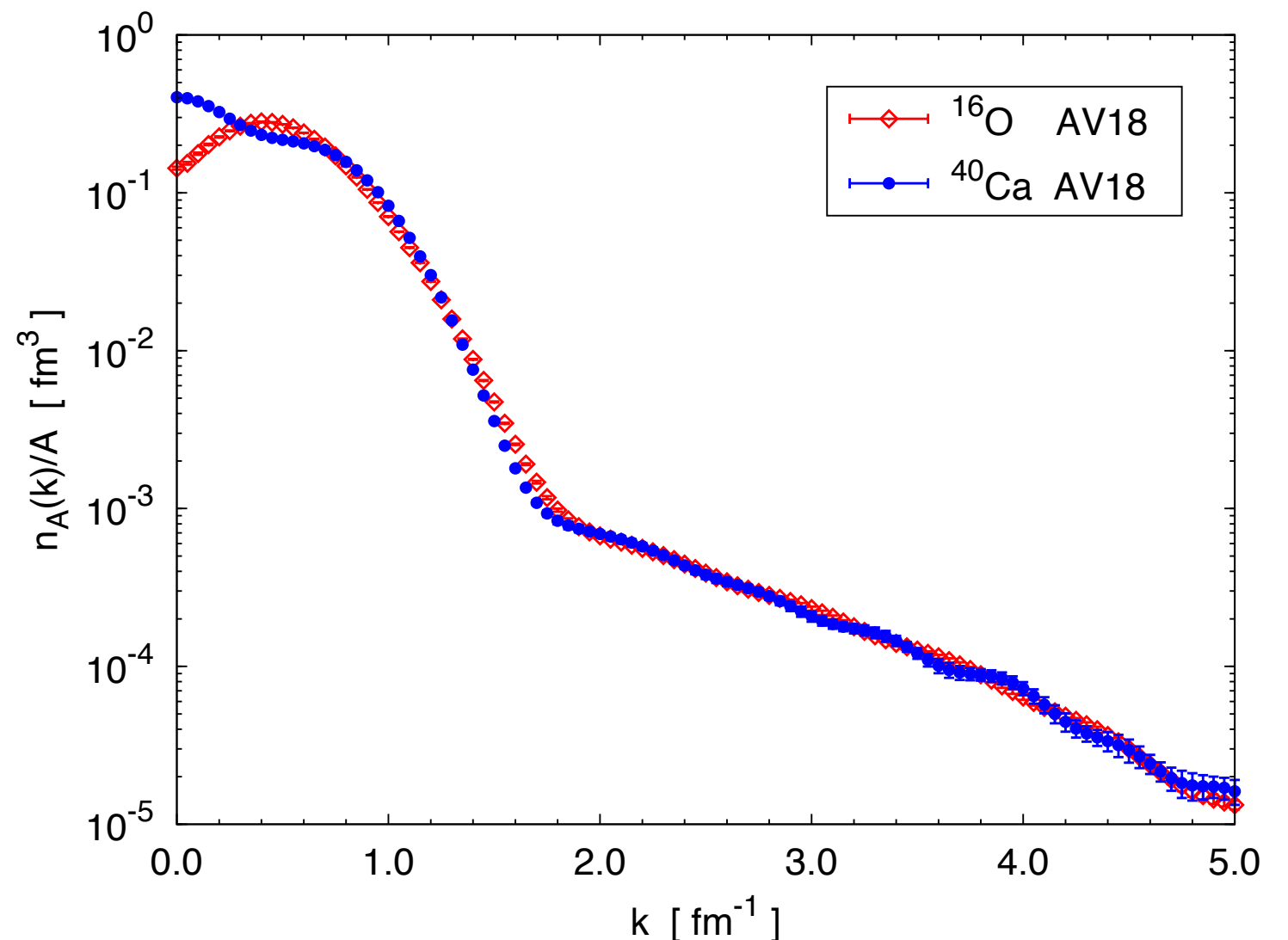
Constraining the spectral function with QMC

The sum rule of the spectral function corresponds to the momentum distribution

$$\int dE P(\mathbf{k}, E) = n(\mathbf{k})$$

- Within Quantum Monte Carlo, we have already computed the momentum distribution of nuclei as large as ^{16}O and ^{40}Ca .
- The energy weighted sum rules of the spectral function can also be computed within cluster variational Monte Carlo

$$\int dE E P(\mathbf{k}, E) = \langle \Psi_0 | a_{\mathbf{k}}^\dagger [H, a_{\mathbf{k}}] | \Psi_0 \rangle$$



Conclusions

- For relatively large momentum transfer, the two-body currents enhancement is effective in the entire energy transfer domain.
- ^4He and ^{12}C results for the electromagnetic response obtained using Maximum Entropy technique are in very good agreement with experimental data.
- Fruitful interplay between quantum Monte Carlo and spectral function approaches. This is possible as they are all based on the same model of nuclear dynamics.
- We are tackling the computation of the neutrino-Argon cross section using different approaches and benchmarking them were possible. However,

It is a very difficult problem, need computing and human time

Path forward

The results we obtained are very nice, but limited and not completely satisfactory

- The continuity equation only constraints the longitudinal components of the current
- The transverse component and the axial terms are phenomenological (the coupling constant is fitted on the tritium beta-decay)
- Two- and three- body forces not fully consistent

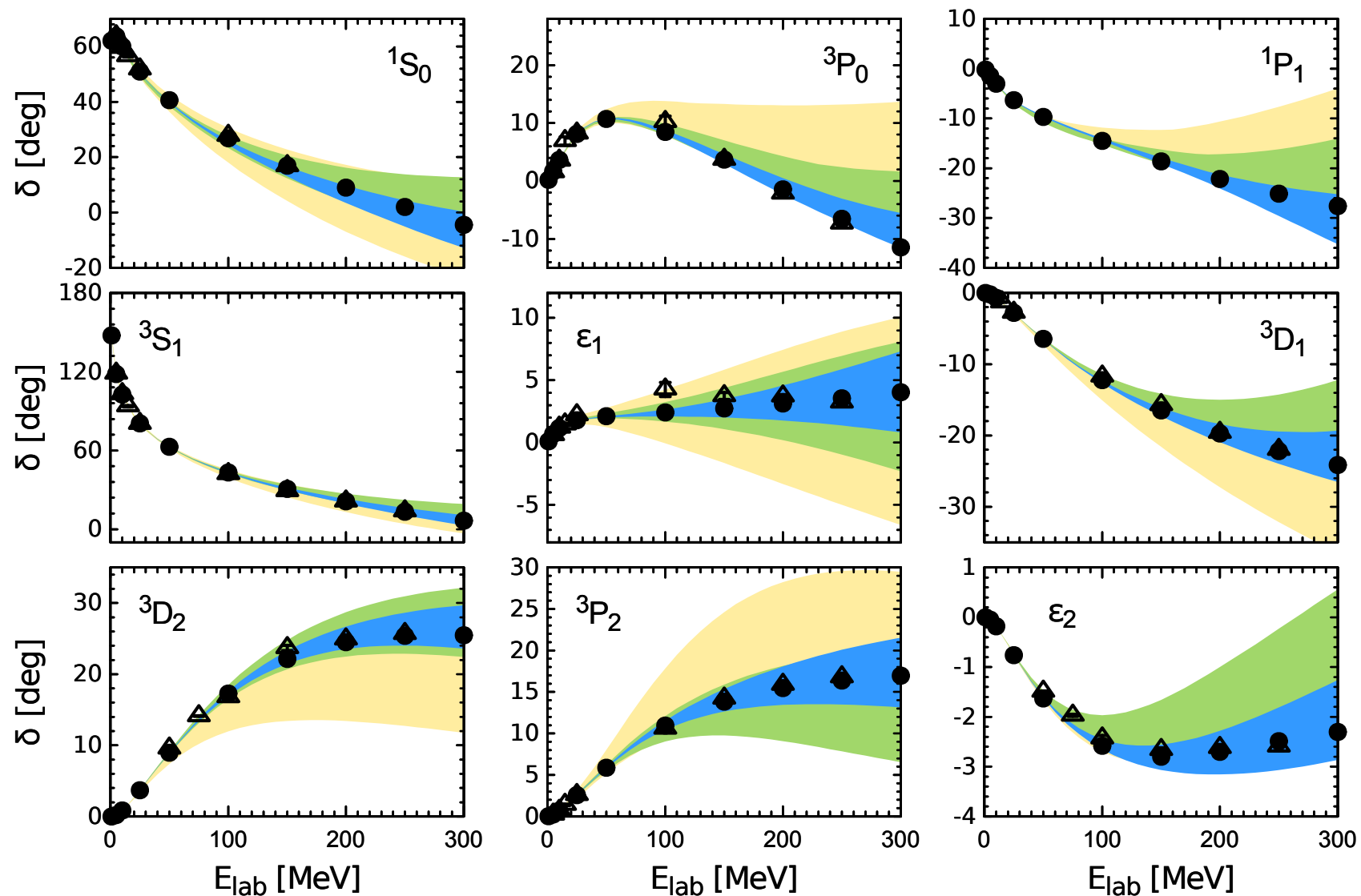
Within this framework, the theoretical error arising from modeling the nuclear dynamics cannot be properly assessed!

Chiral effective field theory (χ EFT) has witnessed much progress during the two decades since the pioneering papers by Weinberg (1990, 1991, 1992)

In χ EFT, the symmetries of quantum chromodynamics (QCD), in particular its approximate chiral symmetry, are employed to systematically constrain classes of Lagrangians describing the interactions of baryons with pions as well as the interactions of these hadrons with electroweak fields

Chiral EFT

χ EFT provides a framework to derive consistent many-body forces and currents and the tools to rigorously estimate their uncertainties, along with a systematic prescription for reducing them.



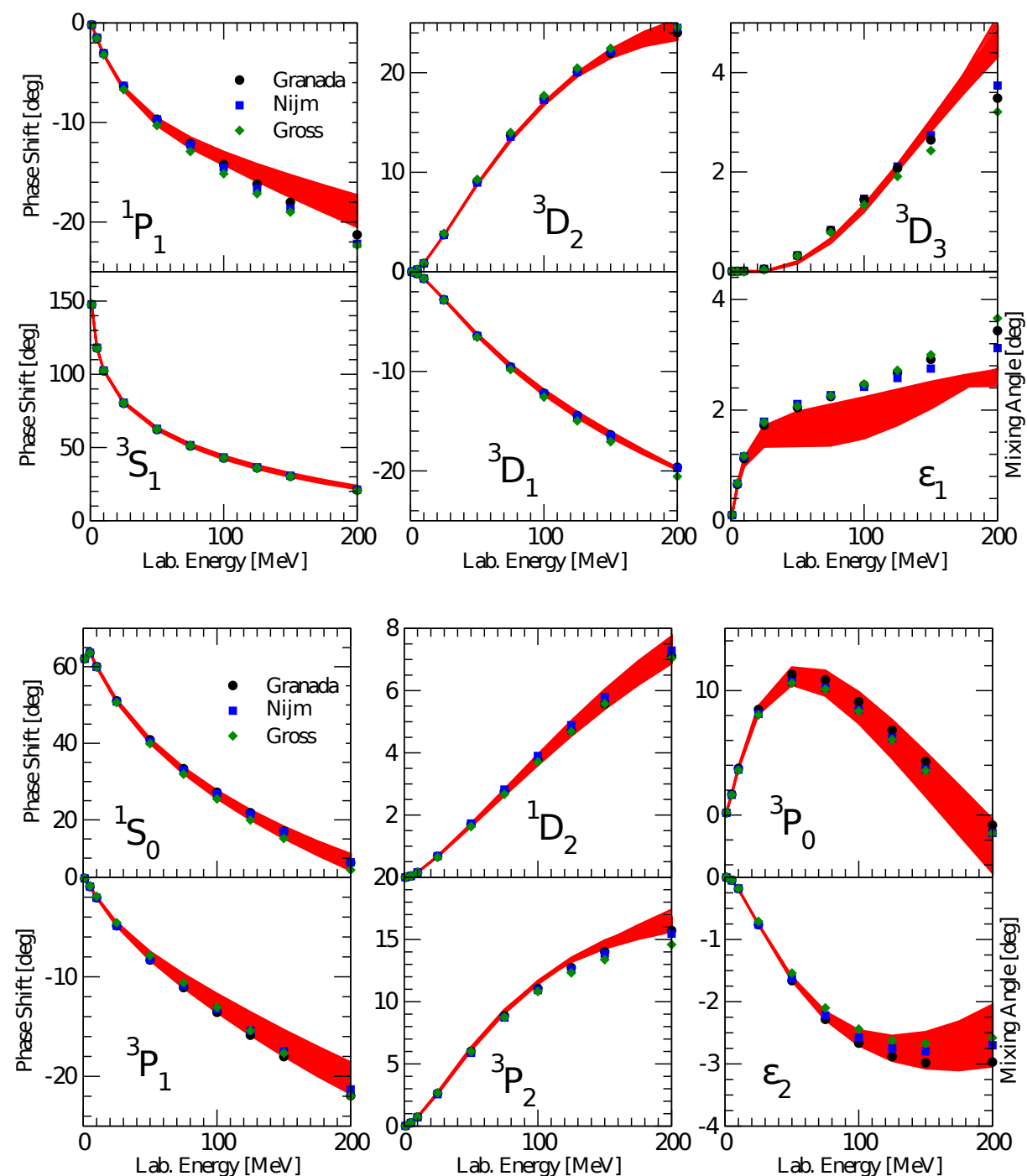
QMC allows to propagate the theoretical uncertainty arising from the nuclear interaction to the response functions

Δ -full local chiral potential

We have complemented the historical “Argonne” approach by considering a local chiral Δ -full potential giving an excellent fit to the NN scattering data that can be readily used in QMC.

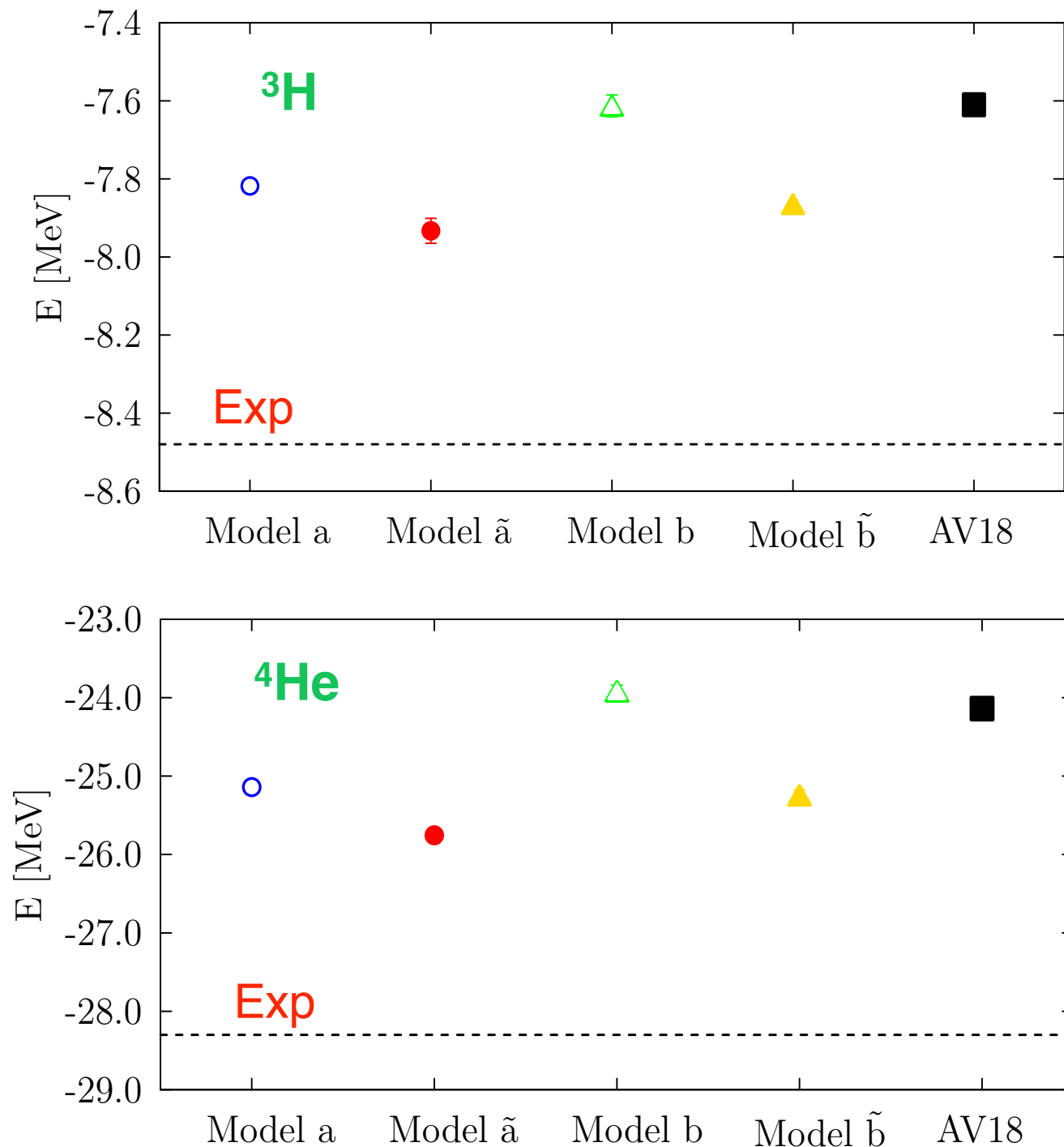
- Closer connection with QCD
- Consistent MEC being constructed
- Reliable theoretical uncertainty estimation

model	order	E_{Lab} (MeV)	N_{pp+np}	χ^2/datum
b	LO	0–125	2558	59.88
b	NLO	0–125	2648	2.18
b	N2LO	0–125	2641	2.32
b	N3LO	0–125	2665	1.07
a	N3LO	0–125	2668	1.05
c	N3LO	0–125	2666	1.11
\tilde{a}	N3LO	0–200	3698	1.37
\tilde{b}	N3LO	0–200	3695	1.37
\tilde{c}	N3LO	0–200	3693	1.40



Δ -full local chiral potential

We computed the binding energy and radii of ${}^3\text{H}$, ${}^4\text{He}$, ${}^6\text{He}$ and ${}^6\text{Li}$ using two different methods



${}^AZ(J^\pi; T)$	VMC	GFMC	GFMC(AV18)
	E_0 [MeV]	E_0 [MeV]	E_0 [MeV]
${}^6\text{He}(0^+; 1)$	-22.58(3)	-24.53(6)	-23.76(9)
${}^6\text{He}(2^+; 1)$	-20.94(2)	-22.87(6)	-21.85(9)
${}^6\text{Li}(1^+; 0)$	-25.86(3)	-27.71(8)	-26.87(9)
${}^6\text{Li}(3^+; 0)$	-22.73(3)	-24.56(8)	-24.11(7)
${}^6\text{Li}(2^+; 0)$	-21.42(3)	-24.04(9)	-22.75(11)
${}^6\text{Li}(1_2^+; 0)$	-20.42(3)	-23.09(11)	-21.99(12)

- Excellent agreement between hyperspherical harmonics and GFMC
- Results compatible with AV18
- A consistent chiral NNN force is under development.

Thank you

Maximum entropy algorithm

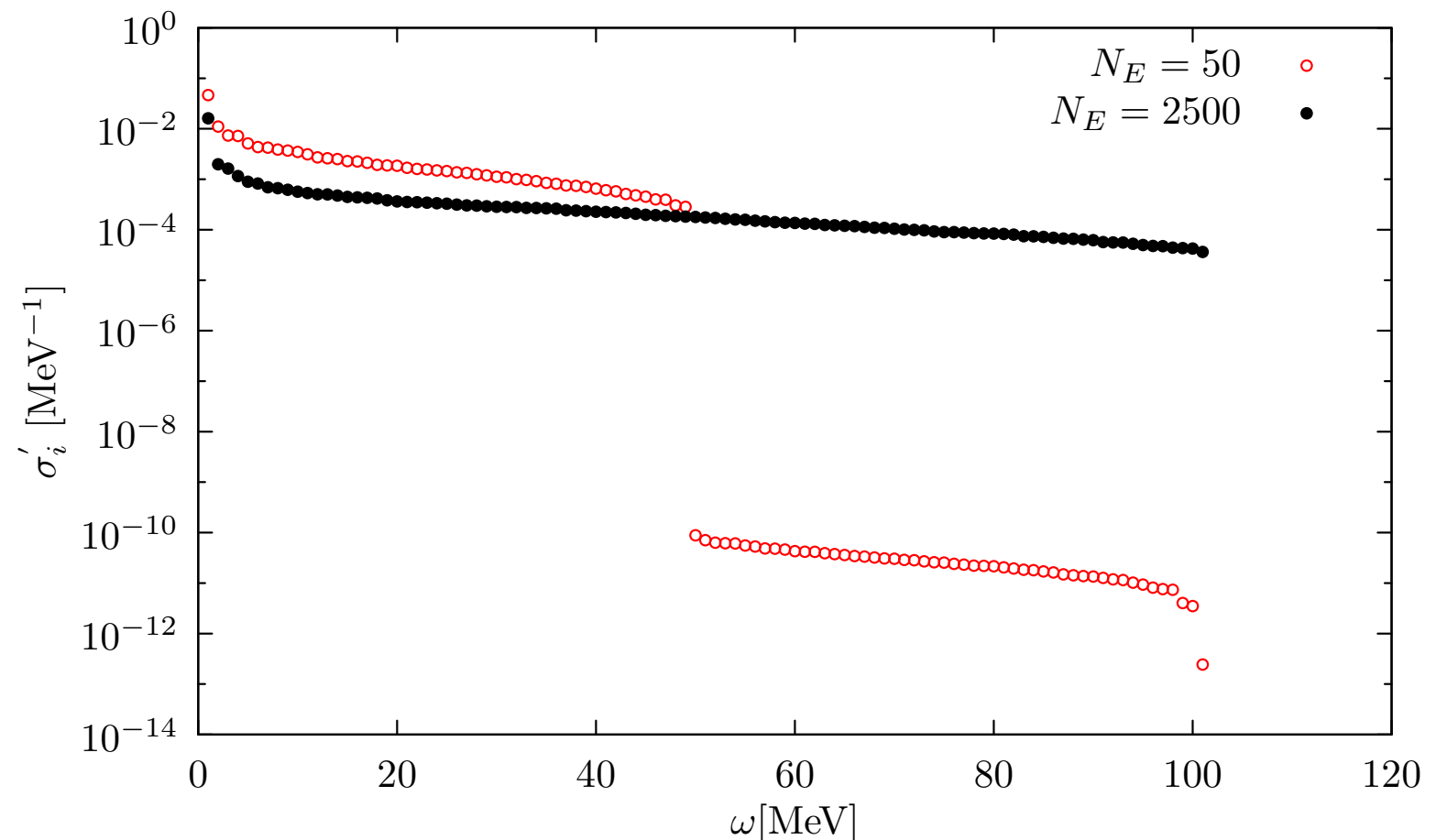
We estimate the mean and the covariance matrix from N_E Euclidean responses

$$\bar{E}(\tau_i) = \frac{1}{N} \sum_n E^n(\tau_i) \quad C(\tau_i, \tau_j) = \frac{1}{N(N-1)} \sum_n (\bar{E}^n(\tau_i) - E^n(\tau_i))(\bar{E}^n(\tau_j) - E^n(\tau_j))$$

- The covariance matrix in general is NOT diagonal, and it is convenient to diagonalize it

$$(\mathbf{U}^{-1} \mathbf{C} \mathbf{U})_{ij} = \sigma_i'^2 \delta_{ij}$$

- If N is not sufficiently large, the spectrum of the covariance eigenvalues becomes pathological.



Maximum entropy algorithm

- The likelihood is defined in terms of the covariance matrix

$$\chi^2 = \sum_{i,j=1}^{N_\tau} (\bar{E}_i - E_i) (C^{-1})_{ij} (\bar{E}_j - E_j) \quad E_i = \sum_{j=1}^{N_\omega} K_{ij} R_j$$

- We rotate both the data and the kernel in the diagonal representation of the covariance matrix

$$\mathbf{K}' = \mathbf{U}^{-1} \mathbf{K} \quad \bar{\mathbf{E}}' = \mathbf{U}^{-1} \bar{\mathbf{E}} \quad \longleftrightarrow \quad (\mathbf{U}^{-1} \mathbf{C} \mathbf{U})_{ij} = \sigma_i'^2 \delta_{ij}$$

- The likelihood can be written in terms of the statistically independent measurements and the rotated kernel

$$\chi^2 = \frac{1}{N_\tau} \sum_i \frac{(\sum_j K'_{ij} R_j - \bar{E}'_i)^2}{\sigma_i'^2}$$

Maximum entropy algorithm

Maximum entropy approach can be justified on the basis of Bayesian inference. The best solution will be the one that maximizes the conditional probability

$$Pr[R|\bar{E}] = \frac{Pr[\bar{E}|R] Pr[R]}{Pr[\bar{E}]}$$

- The evidence is merely a normalization constant

$$Pr[\bar{E}] = \int \mathcal{D}R Pr[\bar{E}|R] Pr[R]$$

- When the number of measurements becomes large, the asymptotic limit of the likelihood function is

$$Pr[\bar{E}|R] = \frac{1}{Z_1} e^{-L[R]} = \frac{1}{Z_1} e^{-\frac{1}{2}\chi^2[R]} \quad \chi^2 = \frac{1}{N_\tau} \sum_i \frac{(\sum_j K'_{ij} R_j - \bar{E}'_i)^2}{\sigma_i'^2}$$

Limiting ourselves to the minimization of the χ^2 , we implicitly make the assumption that the prior probability is important or unknown.

Maximum entropy algorithm

Since the response function is nonnegative and normalizable, it can be interpreted as a probability distribution function.

The principle of maximum entropy states that the values of a probability function are to be assigned by maximizing the entropy expression


$$S[R] \equiv - \int d\omega (R(\omega) - D(\omega) - R(\omega) \ln[R(\omega)/D(\omega)]) \quad \longleftrightarrow \quad D(\omega): \text{Default model}$$

The prior probability then reads

$$Pr[R] = \frac{1}{Z_2} e^{\alpha S[R]}$$

and the posterior probability can be rewritten as

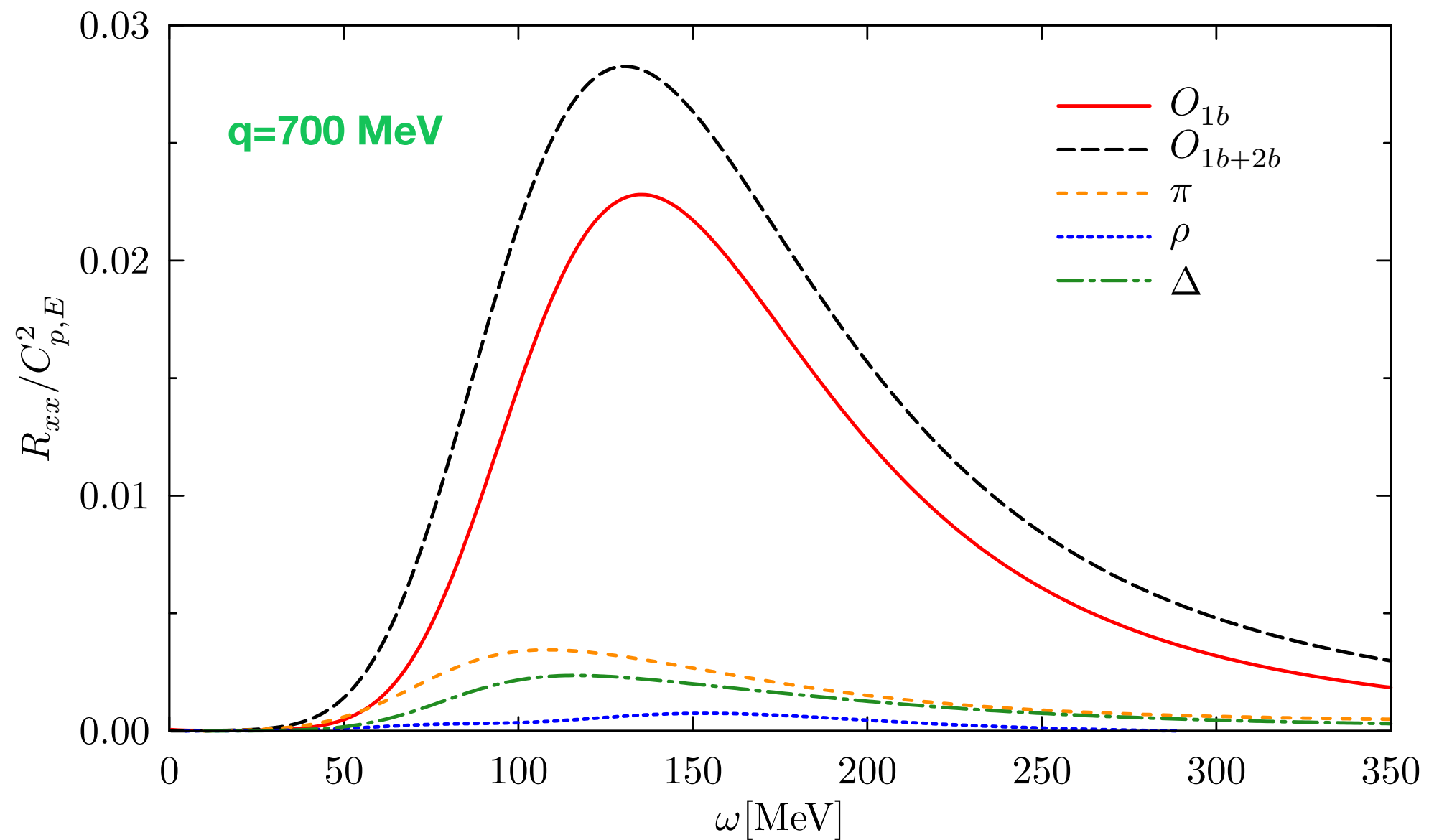
$$Pr[R|\bar{E}] = \frac{e^{-Q[R]}}{Z_1 Z_2 Pr[\bar{E}]} \quad \longleftrightarrow \quad Q[R] \equiv \frac{1}{2} \chi^2[R] - \alpha S[R]$$



Regularization parameter

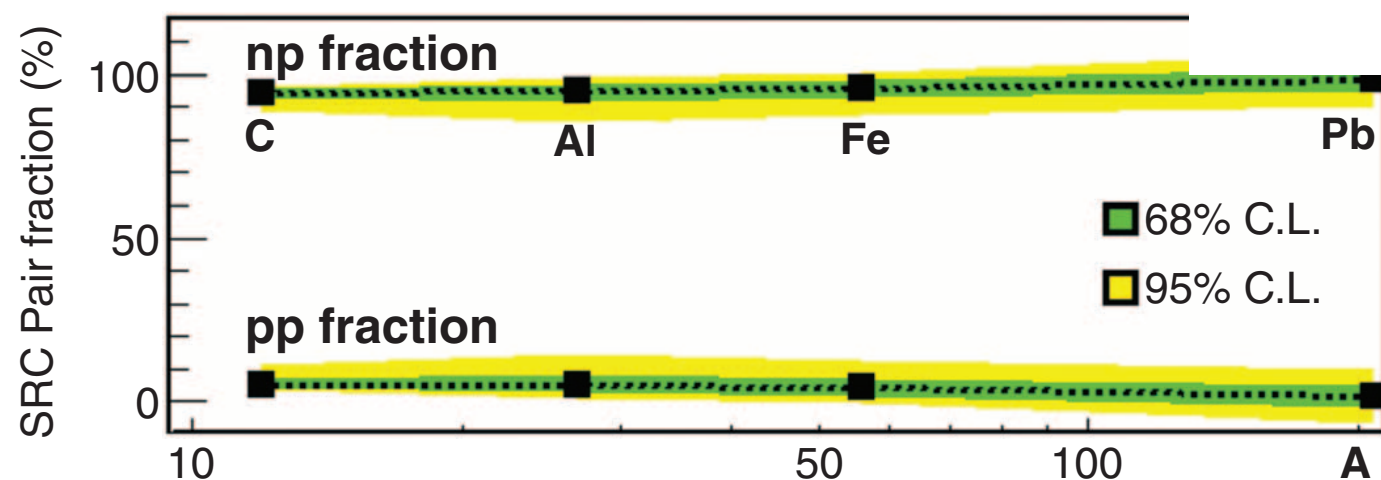
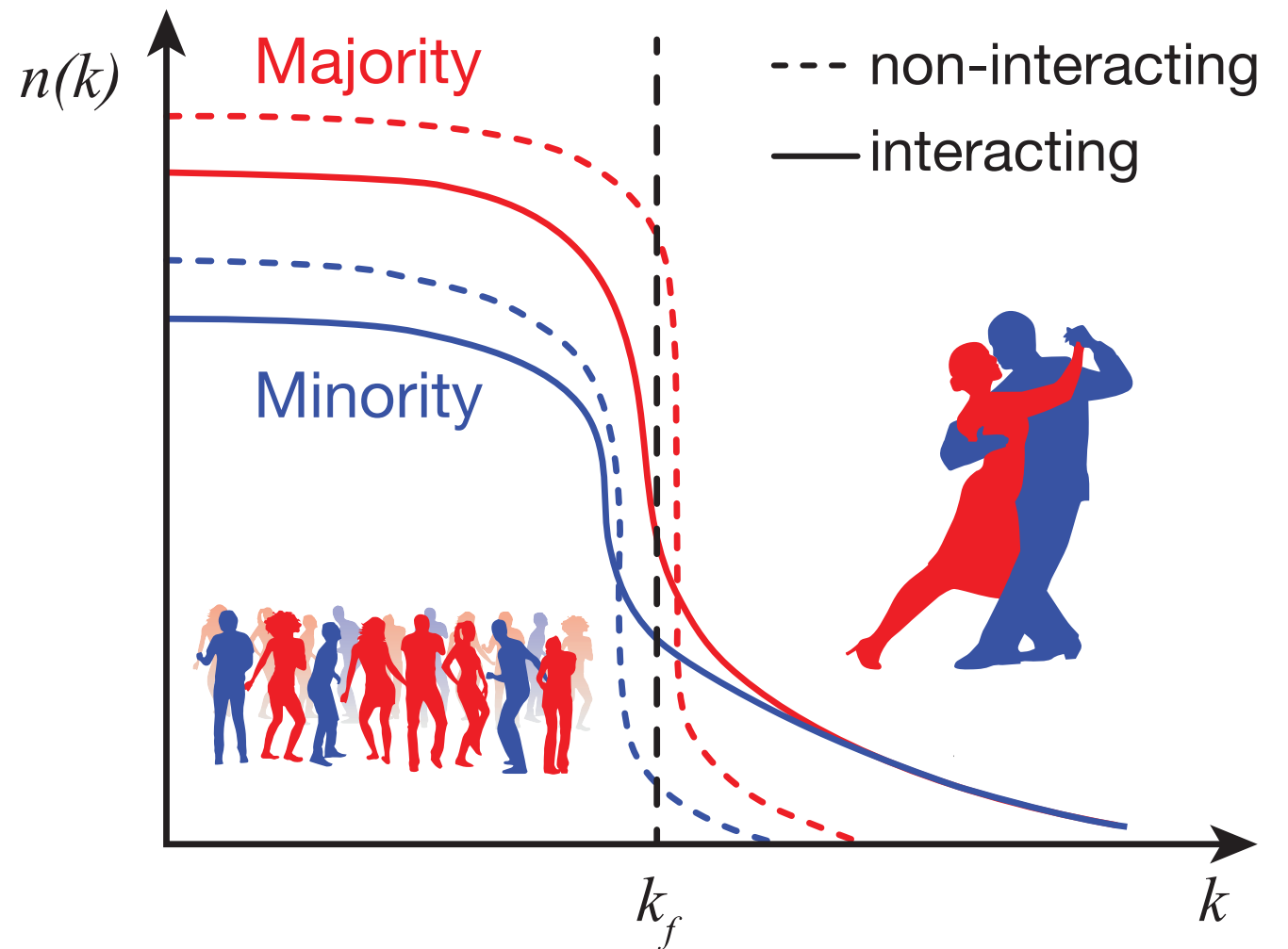
^4He electromagnetic response

The enhancement is driven by process involving one-pion exchange and the excitation of the Delta degrees of freedom



Nuclear correlations

- Nuclear interaction creates short-range correlated pairs of unlike fermions with large relative momentum and pushes fermions from low momenta to high momenta creating a “high-momentum tail.”
- Like in a dance party with a majority of girls, where boy-girl interactions will make the average boy dance more than the average girl



- Even in neutron-rich nuclei, protons have a greater probability than neutrons to have momentum larger than the Fermi momentum.